Microfluidic tools for multidimensional liquid chromatography

Ianovska, Margaryta

Chapter II

Novel micromixers based on chaotic advection and their application —a review

Margaryta A. Ianovska[1,2], Patty P.M.F.A. Mulder[1], Elisabeth Verpoorte[1]

[1]*Pharmaceutical Analysis, Groningen Research Institute of Pharmacy, University of Groningen, The Netherlands*

[2] *TI-COAST, Amsterdam, The Netherlands*

Manuscript in preparation

Abstract

Over the last twenty years, microfluidic technology has received growing interest in a diverse set of fields, including clinical diagnostics, genetic sequencing, chemical synthesis and proteomics, all of which are applications in which mixing plays a central role. However, mixing at the micrometer scale is not easily achieved, due to the dominance of laminar flow, a well-ordered flow regime characterized by fluid streams flowing parallel to each other. Mixing of the dissolved species in two neighbouring solution streams occurs by diffusion only. Given that diffusion is inherently a slow process, and the contact area between laminarly flowing solutions is limited to their contact interface, mixing in such a system is not particularly efficient. Thus, specially designed micromixers that are used to overcome the challenges related to mixing in laminar flows are an important part of many microfluidic platforms. All micromixers ultimately have the same objective, namely to increase contact areas between the solutions to be mixed, in order to shorten diffusion lengths and thus promote more efficient mixing. Chaotic advection is one of the most efficient mechanisms to induce mixing, as it involves the generation of flow patterns which dramatically thin solution layers. In this chapter we describe passive micromixers that were proposed within the last decade, based on chaotic advection and its combination with other mixing principles (e.g. split and recombination (=SAR)). We also discuss the applications of different types of chaotic micromixers in chemical industry, biology, and analytical chemistry. Furthermore, we draw the connection between the design and potential application of recently reported micromixers.

***Keywords**:* Microfluidics; Micromixing; Passive micromixers; Chaotic advection; Combined principles; 3D convoluted channels; Application of the mixers.

1. Introduction

Microfluidic technology has received growing interest due to its promising application as an enabling technology in both industrial and and academic science. The key advantage of microfluidic systems is their small size, which means only small (μL or less) quantities of chemicals are required for the (bio)chemical process or analysis in question.[1] However, if we introduce two liquids from neighbouring inlets into a single microfluidic channel, we will observe that these two streams flow parallel to each other. Even if the microchannel has turns integrated into it, these streams will pass through the turn without any visible mixing occurring (that can continue for a distance of several meters at the flow rates used typically). This regime is called laminar flow and it exists in all micrometer-size channels that operate under flow rates of a few to hundreds of μL/min. In order to use such devices for applications in clinical diagnostics, genetic sequencing and chemical synthesis, where mixing is central to the application, this problem should be first overcome.

Basically, mixing can only be achieved by means of one process, molecular diffusion, which is driven by the gradient formed between highly-concentrated and less-concentrated regions of the molecules to be mixed. Diffusion results in mixing without requiring directed bulk motion, and it is faster if the contact area between two regions is larger. However, in most cases the fluids in the microchannel are introduced by means of a pump at a constant flow rate and the molecules experience advection – molecular mass transfer by bulk motion of fluid that occurs parallel to the direction of the main flow. Due to the laminar flow and constant movement of fluids along the channel, the contact area between two streams is very small and the mixing (diffusion) happens to a minimal degree only at the interface. With an increase in the flow rate (faster movement of fluids), the residence time, or time that molecules spend in the channel, will decrease further, leading to a further decline in both the degree and efficiency of mixing. These effects will be discussed in more detail later (Sec.2.2.).

To overcome a problem with mixing at the microscale, a large number of micromixers have been already developed.[2–4] In general, the purpose of all micromixer designs is to increase the contact area between fluid streams, and in this way, decrease the diffusion length, which makes mixing by diffusion faster. Depending on the basic mixing principle being exploited, micromixers can be divided into either the passive or active category. Active micromixers utilize external energy to perturb flow patterns and achieve mixing. For this, an external power

source has to be integrated into the system, which complicates the fabrication process, and possibly limits the implementation of such devices. In addition, the external forces involved in this type of mixer can negatively influence the samples studied (*e.g.* acoustic waves can degrade synthetic polymers or generate heat, which could lead to unwanted reactions or damage if biological samples are involved).[2] This makes passive micromixers, which do not require an external source of energy beyond that needed for advective flow, a more preferable choice for a wide range of applications.

Passive micromixers can be further classified according to one of the following mixing mechanisms: 1) parallel lamination and 2) sequential lamination (split and recombination (=SAR)), 3) focusing-enhanced (injection), 4) chaotic mixing and 5) droplet micromixers.[2,3] Parallel and serial lamination micromixers first split the inlet flows of the solutions to be mixed into *n* sub-streams and later recombine them into one flow. In the focusing-enhanced micromixer, a single solute flow is split by injecting it into several solvent flows. In chaotic advection, mixing is achieved through generation of chaotic flow patterns formed at an angle to the main flow, as a result of special microchannel geometries. Passive micromixing in droplets exploits an internal recirculating flow field induced by their transport in non-miscible carrier phases.[3]

Micromixers based on chaotic advection provide for fluid stretching and folding over the cross-section of the channel, and are especially effective in microfluidic devices.[1] A relatively new trend in mixer designs is the combination of chaotic advection with the SAR principle, which utilizes so-called 3D convoluted channels that provide efficient mixing over a large range of Reynold numbers (*Re*). In this chapter we will primarily describe and discuss passive micromixers based on chaotic advection. The combination of chaotic advection with other flow processing approaches to achieve fast microfluidic mixing over extended flow rate ranges will also be briefly presented.

In our experience, designing a mixing device can be a time-consuming process, due to the many design parameters that need to be taken into account, as well as the choice of material and fabrication method, depending on the final application. Before endeavouring to make a new micromixer from scratch, one should possess appropriate knowledge and a good understanding of mixing at the microscale, as a lot of designs that work well have been already proposed.[5–28] Our main goal in this chapter is to help the reader in that process by providing him or her with a wide overview of existing micromixers based on chaotic advection and combined principles

that can be applied to a variety of fields. We present reported applications of these devices, which include examples in chemistry, biology and analytical chemistry, to name but a few.

In Section 3 we will discuss the micromixers that have been the most used over the last decade, presented according to geometric classification. We place an emphasis on the channel geometry, flow conditions (described by *Re*) and the mechanism of mixing. In Section 4 we will describe the most common application areas of passive chaotic micromixers with real examples. In the Discussion section we will focus on the link between channel geometry and possible area of application, at different flow conditions known to influence mixing efficiency.

2. Theory

2.1. Viscosity, inertia and the Reynolds number

There are two major forces that play an important role in the microchannels, namely viscous and inertial forces. Both of them can be seen as a measure of resistance. In the case of viscosity, this resistance appears due to frictional shear forces that arise during the motion of molecules. When the fluid moves through a channel as the result of an applied pressure gradient, the molecules of the fluid generally move more quickly in the region around the central axis of the channel than near the walls. This difference in relative motion of the fluid layers results in differing amounts of friction being manifested between layers. Informally, viscosity is said to be related to the "thickness" of liquids and their resistance to flow. For example, water flows more easily than honey because it has a lower viscosity than honey. Inertia, on the other hand, is the resistance of a volume of fluid to change its state of motion or its velocity (the fluid prefers to continue moving in a straight line at a constant velocity). The magnitude of the inertial force in a fluid flow depends on the mass of the fluid, increasing as fluid mass increases.

The interplay of these two forces determines the flow regime at a given flow rate in any type of channel and can be expressed as the Reynolds number (see Equation 1). The flow regimes that govern the behaviour of fluids in channels can be broadly divided into laminar or turbulent. The Reynolds number predicts the range of flow rates at which flow in a microchannel changes from laminar to turbulent. It is expressed as a measure of the ratio of inertial forces to viscous forces for a given set of flow conditions:

$$Re = \frac{\text{Inertial Forces}}{\text{Viscous Forces}} = \frac{v d_h \rho}{\mu} \quad (1),$$

where d_h denotes the hydraulic diameter of the channel (see Eqn. 2), v is average linear velocity (m/s), ρ equals the density of the fluid (kg/m^3) and μ represents the dynamic viscosity of the fluid (kg/(ms)). In case of heterogeneous flow, an average density and an average viscosity based on the proportion of each fluid in the mixture are calculated. The fully turbulent regime starts at Re > 3000 (depending on channel diameter).

Using the Reynolds number (*Re)* makes it is possible to compare different designs under the same flow conditions.

The hydraulic diameter can be calculated with the following equation:

$$d_h = \frac{4A}{P} \quad (2),$$

where *A* is the cross-sectional area of the flow (mm^2) and *P* is the perimeter of the cross-section (mm).

For a channel with circular cross-section the hydraulic diameter is calculated using the radius of the circular pipe (*r*, mm), yielding the following familiar relationship:

$$d_h = \frac{4\pi r^2}{2\pi r} = 2r \quad (3),$$

The hydraulic diameter of a rectangular duct is:

$$d_h = \frac{2wh}{w+h} \quad (4),$$

where *h* is the channel height (mm) and *w* is the channel width (mm).

2.2. Forms of mass transport to achieve the mixing

In general, there exist four types of mass transport in miccrochannels, namely molecular diffusion, eddy diffusion, advection, and Taylor dispersion.[29] Eddy diffusion is the transport of large solutes by turbulent flow, where turbulent flow is characterized by chaotic changes in flow velocity. However, the dominance of viscous forces at the microscale at the flow rates typically used makes turbulence difficult to achieve ($Re \leq 2000$) and, hence, this type of mixing is not relevant for micromixers.

Taylor dispersion refers to the dispersion of solutes at the front of an advancing solution flow in a microfluidic channel. When a new solution is introduced into an already-filled microchannel under pressure-driven flow conditions, the solution front quickly adopts the parabolic velocity profile in the channel. As a result, the front of the new solution is drawn out into the back end of the solution in front of it, creating concentration gradients of dissolved compounds across the channel in a direction perpendicular to flow. Diffusion of species between streamlines having different velocities (due to the parabolic profile of the flow),[30] serves to further smear out the sharp concentration profile at the solution front. Because Taylor dispersion occurs in the direction of flow, it can be seen as an interplay between advection and diffusion. In the situation when the microchannel is already fully filled with a given solution, and no new solutions need to be introduced, Taylor dispersion no longer is a parameter, which needs to be taken into consideration when describing flows and concentration gradients. In fact, concentration gradients will cease to exist once advective flow has served to fill the microchannel entirely with one solution having a constant composition. However, it is worth

noting that at the interface between two fluid streams, Taylor dispersion is also dictated purely by molecular diffusion.

The most important forms of mass transport at the microscale remain molecular diffusion and advection. Molecular diffusion involves the random motion of molecules, whereas molecular transport by advection sees molecules being carried in bulk flow. Diffusion is a mass transfer phenomenon that causes the distribution of dissolved (bio)chemical species to become more uniform in space as time passes. The driving force for diffusion is the thermal motion of molecules, where molecules migrate from a region of high concentration to a region of low concentration. Fick's first law of diffusion states that the magnitude of this molecular flux is proportional to the concentration gradient thus formed, as expressed in the following equation:

$$J = -D\nabla n \quad (5),$$

where J is the diffusion flux per unit area per unit time (mol/(m^2×s)), D is the diffusion coefficient (m^2/s) and ∇n represents the relevant concentration gradient (mol/m^4). The diffusion coefficient, D, is a measure of the rate of the diffusion process. The average distance that a molecule travels by diffusion in a given amount of time can be calculated using the Einstein-Smoluchowski equation, given below, which was derived from Fick's law of diffusion by the two scientists after which it is named.

$$d_{diff} = \sqrt{2Dt} \quad (6),$$

In this equation, d_{diff} is the distance a dissolved species travels in a time, t (s). Usually, diffusion is a very slow process. For instance, a molecule of glucose with a diffusion coefficient of 5 × 10^{-6} cm^2/s requires more than 27 h to travel a distance of 1 cm (the total path-length).

Diffusion is superimposed on advection, the mass transport that occurs in a direction parallel to the main flow as a result of dissolved molecular species being carried by the flow. Advection determines the flow conditions under which diffusion takes place. In fact, advection is not very useful in microfluidics for the mixing process, given the predominance of laminar flow at the flow rates typically used in microfluidics (μL/s to μL/min). However, advection that occurs in directions that are not parallel to the net flux of the solution, secondary flows also known as chaotic advection, can facilitate mixing dramatically.[1] In chaotic advection simple regular velocity fields produce chaotic molecular or particle trajectories.[31] This results in an exponential growth of the interfacial area and an accompanying decrease in the thickness of the fluids layers over which diffusion must occur to complete homogenization of two or more

solutions. Thus, chaotic advection is a very promising mechanism to improve mixing at the microscale.[2]

It is important to note that chaotic advection is not turbulence. For a flow system under steady state, the velocity components in chaotic advection at each point in space remain constant over time, while the velocity components in turbulent flow vary over time at each point in space.[1] A necessary condition for chaos is that streamlines should cross each other at different times, causing particles to change their paths. Thus, chaotic advection can occur in a time-periodic flow or a spatially time-independent periodic flow.[1] The first type can be implemented by setting boundaries into motion through application of external forces (e.g. electric field). These micromixers fall into the active category, and are based on effects such as electrokinetic instability, EKI, a phenomenon which ca be induced in a microchannel using an applied electric field.[32,33] Chaotic advection in a spatially time-independent periodic flow can be achieved by using 2D curved channels, for example, which will be described in Section 3.1.

Many authors[20,22,34–36] report that there exists a critical value of the Reynolds number (Re_{cr}) for every micromixer based on chaotic advection. Below this critical value, mixing is dominated by diffusion and because the *Re* is proportional to the linear velocity in the system (*i.e.* flow rate), the mixing efficiency is reduced with increase in flow rate. Above Re_{cr} the mixing process is advection-dominated and mixing efficiency increases with increase in flow rate. A probable explanation for this observation is that at low flow rates, the strength of these secondary flows is not sufficient to significantly disturb the laminar flow profile, and mixing by diffusion occurs between two neighbouring parallel streams. When secondary flow patterns become more pronounced at higher flow rate, mixing by diffusion is facilitated by resulting increases in contact area and thinner solution streamlines. Each particular micromixer design has its own critical value of *Re*, above which mixing is especially efficient. For the end-user looking for an appropriate mixer for a specific application, the critical value of Reynolds number should be an important indicator whether a chosen micromixer design will work in the most efficient way under the required conditions of the particular application.

3. Passive micromixers based on chaotic advection

In this section we will describe designs and mixing mechanisms of the mixers that have been proposed within the last decade. The classification of these micromixers is based on their geometry and includes simple channels (spiral, zig-zag and serpentine), obstacles or wall modifications, and 3D convoluted channels. The possible mechanism of mixing depends on the channel geometry. Flow conditions (described by *Re*), under which the mixer is operated, dictate the type of phenomenon that governs mixing and, thus, the efficiency of mixing. Thus, each design can provide different mixing performances at different *Re*.

3.1 Simple geometries: spiral, zig-zag and serpentine channels

The easiest design for creating chaotic advection is the T-mixer, where two streams collide at a T-junction. Due to the sharp 90° angle at the entrance, the inertial force is large enough to cause vortices at the junction (so-called Dean vortices), which lead to chaotic advection.[37] T-mixers have been investigated extensively by many researchers.[38–40] However, the efficient application of T-mixers require *Re*>150, which is Re at which vortices inside the T-mixer become asymmetric and real chaotic advection occurs.[1] Thus, many research groups used the T-junction for introducing streams of liquids in combination with other channel modifications, for instance, the spiral[6,35] zig-zag-shaped[36] and serpentine[22] microchannels. In these designs, similar to the T-mixers, the chaotic advection is induced by the appearance of Dean vortices when the fluids experience centrifugal effects when traveling along a curved path of the pipe or at turns in the channel.[6] Dean flow can be intensified by introducing larger numbers of repetitive turns (Fig. 1A), and mixing by chaotic advection will be improved when the flow rate used is increased.

Sundarsan *et al.*[35] tested mixing in spiral channels (Fig. 1A) using five different designs (the four-arc, six-arc, eight-arc and ten-arc spiral channels) for Reynolds numbers between 0.02 and 18.6. The mixing efficiency of all designs improves with increased flow rate (*Re*>10) and with increase in length of individual spiral contours together with decrease of their curvature radius. This effect illustrates the correlation between mixing efficiency and the flow rate (*Re*, *De*). Li *et al.*[5] designed a planar labyrinth micromixer (PLM) (Fig. 1Ba) consisting of ten successive in-line "S-shaped" mixing units (Fig. 1Bb) that are compactly arranged within a confined circular area. Using such micromixers the range of Reynolds number, at which efficient mixing occurs, can be expanded to *Re* 30. A design with a short straight channel

between two consecutive semicircles arranged with a 180°-turn provides continuous rotation of the fluid, repeatedly distorts the interface between two streams, and breaks up unmixed regions due to a complete position switching of the two streams.

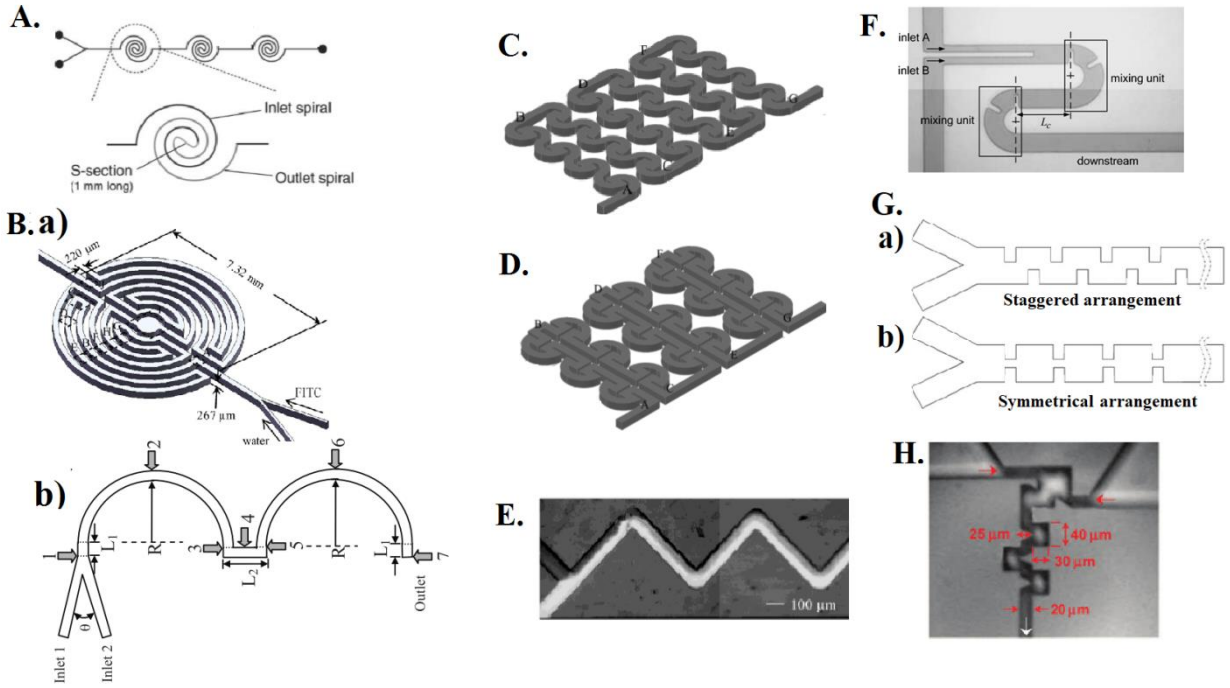

Figure 1. Passive micromixers with simple geometries: (A) The spiral channel network incorporating three mixing sections (Modified from[35]); (B) (a) a scheme of the planar labyrinth micromixer (PLM) with (b) "S-shaped" mixing unit (Modified from [5]); (C) ILSC mixer and (D) Ω mixer (Modified from[6]). (E) Microscopy image of a zig-zag microchannel (Taken from[36]; (F) C-shaped micromixer micromixer with baffles (Taken from[27]); (G) Mixer with (a) staggered and (b) symmetric obstructions along the microchannel (Modified from [22]; (H) A passive alcove-based mixer (Taken from[23]). See Table 1 for geometric dimensions.

Recently, inspired by the mixing results in the spiral channels, Al-Halhouli *et al.*[6] presented computational simulations and experimental results for two new mixers composed of units shaped as interlocking-semicircle (ILSC) and omega (Ω) channels. The ILSC mixer (Fig. 1C) consists of several mixing modules, which are composed of two offset mirrored interlocking semi-circles (ILSC) whereas the second design consists of series of Ω-shaped modules (Fig. 1D). Both designs enable a simultaneous rapid 90°-change in the flow direction (and the direction of Dean vortices formed) four and six times within each Ω- and ILSC mixing module, respectively. Both micromixers can be used over the entire range of $0.01<Re<50$; however, complete mixing is achieved only at $Re>10$. It should be mentioned that the strength

of Dean vortices in the Ω design is expected to be less than those in the ILSC design for a given Reynolds number, because the Ω-mixer has 1.67-times larger mean radius of curvature.

Another simple design that was exploited decades ago, is a zig-zag microchannel (Fig. 1E), where periodic turns cause chaotic advection. Mengeaud *et al.*[36] made simulations in the Reynolds number range of 26-267. They found that there exists a critical Reynolds number of 80, under which the mixing relies entirely on molecular diffusion. At higher *Re*, mixing was improved by recirculation generated at the channel turns.

Tsai and Wu [27] introduced radial baffles to the curved microchannel and named this design a curved-straight-curved (C-shaped, CSC) micromixer (Fig. 1F). Dean vortices due to the curved channel appear after the baffles, and the converging-diverging flow profile between the baffle and the channel wall enhance mixing at $Re \geq 27$.

Another approach was taken by Sahu *et al.*[22], who investigated mixing in a microchannel integrating short narrow channel sections. Two types of obstructions were studied, namely a staggered (Fig. 1Ga) and symmetric (Fig. 1Gb) arrangement. It was observed that the staggered arrangement provided slightly higher (5%) mixing performance due to the presence of a cross-stream velocity component. It was shown that mixing efficiency increases quadratically with the number of obstructions due to increased residence times in the obstruction region. A larger depth and width of the obstruction leads to larger turns of the flow, introducing larger secondary flow that leads to higher mixing efficiency. The pressure drop is observed to be significantly higher in the case of symmetric arrangements. In this type of mixer, a relatively high critical value of $Re_{cr} \sim 100$ was found.

A sophisticated design termed an “alcove-based mixer” was proposed by Egawa *et al.*[23] (Fig. 1H). The mixer consists of a T-junction, followed by three repeats of an alcove or cavity, adjusted to the channel and arranged in a zig-zag manner. This mixer is capable efficiently of mixing solvents with different viscosities (1.04-1.17 cP), due to recirculation of solution within the alcoves to promote fluid mixing.

3.2 Microchannels with wall modifications

Another simple way to induce transverse flow in the microchannel is to insert obstacles or to modify the channel wall with grooves. Special attention will be paid to mixers with grooves fabricated in the channel walls.

Placing obstructions within a microfluidic channel offers a simple approach to enhance mixing by chaotic advection. Obstacles alter the direction of flow, and the resulting swirling flows and recirculation create transverse mass transport. The barriers are placed asymmetrically in an alternating way inside the microchannel[41] to provide even more chaotic flow patterns, due to changing flow directions that force fluids to merge.[42,43]

Wang *et al.*[42] numerically investigated different layouts of cylindrical pillars in a mixing channel. This work showed that obstacles cannot generate eddies or recirculation at low Re. However, mixing performance can be improved at high Reynolds numbers ($Re \geq 200$). One of the important findings was that an increase in the number of obstacles in the channel led to the enhancement of the mixing. Later, Chen *et al.*[44] reported a microfluidic mixer containing a high-density array of pillars (Fig. 2A) that can provide fast mixing at very low Reynolds numbers ($Re \leq 1$). The micropillars cause multiple splitting and reunification of laminar flows in the channel. At a low flow rate of 0.1 μL/min, almost complete mixing was obtained due to this ‘‘split-and-recombination’’ effect (discussed more in Section 3.3), that decreases the thickness of each fluid layer and provides shorter characteristic diffusional lengths. However, this effect is highly reduced at higher flow rates and more clusters of obstructions are needed for complete mixing. When the flow rate was increased to 5–15 μL/min, the mixing process starts to be dictated by chaotic advection, and mixing performance is slightly enhanced. The mixer was tested for mixing solutions with different viscosities (phosphate-buffered solution, gold nanocolloids and 20% glycerol with Rhodamine 6G) at various flow rates (0.1-10 μL/min). As expected, glycerol/Rhodamine 6G, due to its higher dynamic viscosity (1.76 cP), shows a relatively lower mixing efficiency than the other solutions, and requires a distance of 35 mm compared to 21 mm with phosphate buffer solution to obtain completet mixing.

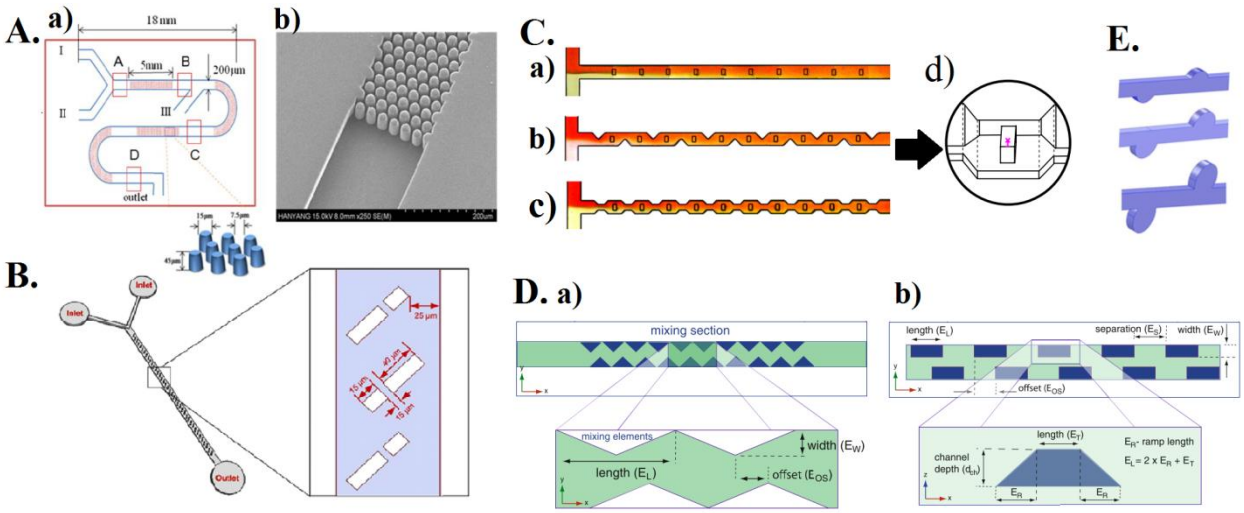

Figure 2. Micromixers with obstacles in the mixing channel: (A) A pillar obstruction micromixer: (a) schematic diagram and (b) SEM image of micropillars in poly(dimethylsiloxane)(Modified from[25]); (B) An obstruction-based micromixer with rectangular ribs (Taken from[26]); (C) T-shaped (a) simple, (b) wavy and (c) converging–diverging micro-channels with rectangular ribs and (d) magnified rectangular rib placed on the channel floor (Modified from[17]); (D) Micromixer with incorporated 2D and 3D baffles (a) 2D mixer with triangle-shaped mixing elements and (b) 3D mixer with trapezoidal mixing units (Modified from[28]); (E) Mixer with cylindrical alcoves (Modified from[24]). See Table 1 for geometric dimensions.

Another obstruction-based micromixer with optimized rectangular ribs was reported by Bhagat *et al.*[26](Fig. 2B). It provides ~90% fluid mixing within 5 mm and is capable of achieving particle dispersion with a wide range of particle sizes (190 nm - 1.9 μm), showing a 30% increase in particle dispersion over a modified Tesla design[45] (discussed in Section 3.3).

Hsieh and Huang [17] proposed mixers that can work at very low *Re* ($0.027 \leq Re \leq 0.081$) (Fig.2C). Several T-shaped designs with rectangular ribs with simple (T_r) (Fig.2C-a), wavy (T_{wr}) (Fig.2C-b) and converging–diverging microchannels (T_{cdr}) (Fig.2C-c) were proposed. Although all micromixers perform better at low *Re*, there was an established performance superiority as follows: $T_{wr} > T_{cdr} > T_r$. The periodically positioned ribs improve mixing performance by altering the flow direction. However, the fact that better mixing is achieved at lower *Re* indicates that the mixing is governed mainly by diffusion, which requires longer residence time to occur. Probably, as in many other cases, there exists an Re_{cr}, above which the mixing will become more efficient by increasing the flow rates.

Conlisk and Connor[28] designed 2D- and 3D micromixers with triangle- (Fig. 2Da) and trapezoidal-shaped (Fig. 2Db) baffles. The characterization within *Re* range 0.1–20 showed (Re_{cr} = 1.0) that 90% of the mixing was achieved in 32 and 7 mm for the 2D and 3D mixer

respectively. The mixing is enhanced due to the focus-and-diverging effect. The 3D mixer showed a significant increase in mixing efficiency (82% mixing homogeneity compered to a simple T-mixer) by introducing transverse flow recirculation due to the shape of 3D baffles.

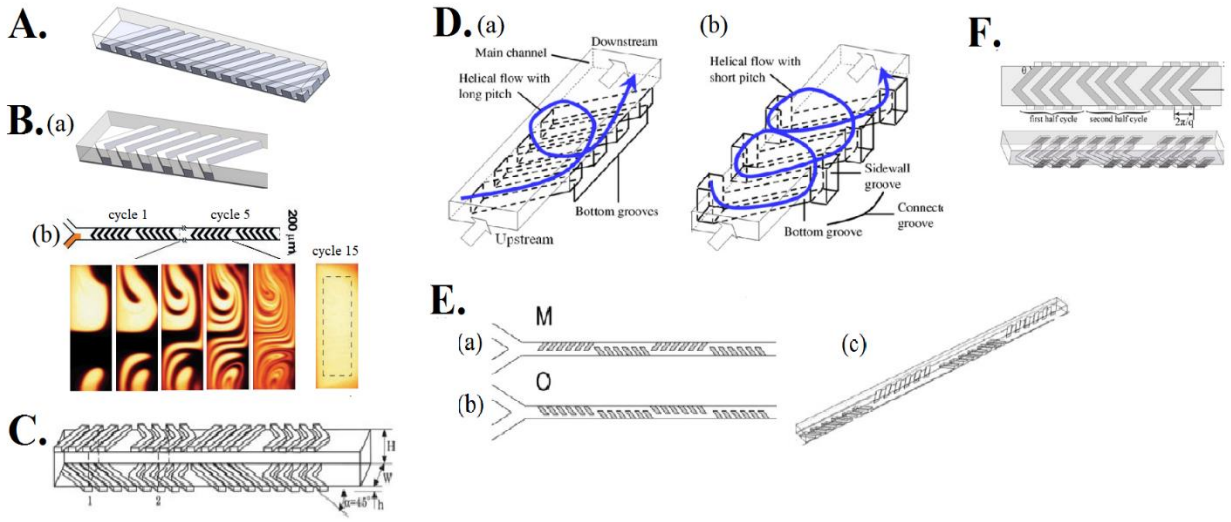

Figure 3. Micromixers with structures on channel walls: (A) Schematic diagram of slanted groove micromixer (SGM) and (B) (a) Staggered herringbone mixer (SHM) and (b) chaotic mixing patterns in the channel (Modified from [52]); (C) Micromixer with both slanted and herringbone grooves (Taken from[53]); (D) Connected-groove micromixer (CGM): (a) CGM-1; (b) CGM-2 (Modified from[34]); (E) Mixer with alternating slanted ridges on the top and bottom of the channel: (a) Slanted Ridge Mixer Mirrored (SRM-M) and (b) Slanted Ridge Mixer Opposite (SRM-O) and (c) 3D view (Taken from[7]); (F) Three-dimensional staggered herringbone mixer (3D SHM) (Taken from[8]). See Table 1 for geometrical dimensions.

Recently, Wang *et al.*[24] proposed designs with cylindrical alcoves extending from microchannel walls (Fig. 2E) that varied in radius. In general, the design with smaller cylindrical alcoves gave a 15% and 37%-increase in mixing performance compared to the straight channel for *Re* 0.1 and 100, respectively. On the other hand, with the increase in *Re* the efficiency of mixing decreased in all the mixers.

Modifying the channel wall is a powerful tool for creating chaotic advection, especially at low *Re* numbers. This approach benefits from the low pressure drop and relatively easy fabrication techniques due to the planar structure.[46] Probably the most well-known examples of patterned a wall of the channel are those micromixers incorporating slanted (SG) (Fig. 3A) and staggered herringbone (SHG) grooves placed on the bottom wall (Fig. 3B, 3C). They have been studied extensively.[47–51]

Grooves can generate transversal secondary flow similar to Dean vortices.[52] In a slanted-groove-micromixer (SGM, Fig. 3A) flow over the groove array assumes a chaotic helical or

corkscrew pattern, in which two solution streams twist around each other close to the bottom of the channel. Fluid elements are stretched in a transverse direction due to the oblique position of the groove with respect to the channel walls. This increases the contact area between two adjacent solutions dramatically and facilitates mixing by diffusion. A detailed description of the mechanism is given elsewhere.[51] However, helical flow in a channel alone does not give rise to chaotic mixing. In order to induce chaotic advection, it is necessary to superimpose different recirculation patterns.[54] This can be achieved with array of staggered herringbone grooves (SHG) (Fig.3B), as described by Stroock *et al.*[52] These structures generate a pair of counter-rotating vortices that stretch and fold the mixing liquids, reducing the striation thickness significantly.[50] Repetition of these patterns leads to chaotic advection. A detailed description of the mechanism can be found elsewhere.[47,50,51]

A variety of designs have been derived from this basic concept. For instance, Howell *et al.*[53] proposed a micromixer with both slanted and herringbone ridges, whereas some designs employ grooves on both top and bottom walls (Fig. 3C) [53,55] or on the side and top walls (Fig. 3D-3E).[8,34] The design proposed by Howell *et al.*[53] (Fig. 3C) with both slanted and symmetric herringbone ridges (chevrons) aims to improve the mixing using the combined mechanism: the chevrons generate two equally-sized vortices that drive fluid upward in the center of the channel and downward toward the sidewalls. On the other hand, the SG creates two vortices, one above the other. Such a design allows the formation of a pair of counter rotating vortices in vertical and horizontal planes, which creates far more rapid mixing than previous designs. Later, Floyd-Smith *et al.*[55] showed that grooves on the top and bottom of channel improve mixing by 10% over micromixers with grooves placed only on one channel wall.

In designs where connected grooves are composed of bottom grooves and sidewall grooves conjoined across the adjacent walls, the sidewall grooves assisted in inducing an intensive helical motion. This situation was observed in connected-groove micromixer with slanted grooves on the bottom and sidewall grooves (CGM, Figure 3D).[34] From the bottom grooves the fluid is guided along the sidewall grooves, then to the top and back to the main stream. Such design can increase the helical intensity by 20%. Recently, Van Schijndel *et al.*[7] proposed a mixer with alternating slanted ridges on the top and bottom of the channel (Fig. 3E). Adding mixing elements to both walls promoted lateral mass transport and assisted in the formation of advection patterns, which increased mixing efficiency. Lin *et al.*[8] theoretically and experimentally showed a micromixer with staggered herringbone grooves patterned on both

bottom and side walls (3D Staggered herringbone mixer, SHM, Figure 3F) that reduced the mixing length by almost half as compared with the originally reported SHM mixer.[52]

The simulations confirmed that the flow pattern in the mixers with staggered herringbone grooves is almost independent of Reynolds number.[1] SHG improve mixing for a wide range of *Re* from 1 to 100.[34,52] However, a dependence of efficiency of mixing on flow rate (different *Re*) is observed, implying the existence of an Re_{cr} (that was mentioned before) can be observed for grooved mixers as well. It was shown that in the connected-groove micromixer,[34] the distance required for complete mixing for $Re>10$ decreased with increasing flow rate because the inertial forces start to dominate over viscosity.

3.3 3D convoluted channels (combined principles)

As shown previously in this Section, simple channels can generate chaotic advection at higher *Re*. However, the mixing at low *Re* (<1) remains a problem in these designs. To overcome this, a large number of novel three-dimensional serpentine (3D convoluted, 3D twisted) designs based on planar micromixers (Section 3.1 and 3.2) have been proposed over the last decade. The mixing in such micromixers is enhanced by the superposition of several mechanisms, mostly the combination of chaotic advection and the splitting-and-recombination principle (SAR). The complex 3D geometry of such mixers causes continuous splitting, recombination and collision of flows at the same time. In general, chaotic advection in this type of micromixer can be induced at high flow rates, $Re>70$, while the SAR mechanism works well at lower *Re*, decreasing the operational range of such mixers to $5<Re<30$. Due to the combination of mixing principles, the distance required for complete mixing in these mixers is much shorter than in mixers based only on chaotic advection.

A good example of such a micromixer is the serpentine laminating micromixer (SLM) developed by Kim *et al.*[56] The mixer consists of ‘‘F’’- shaped units arranged in two layers (Fig. 4A) that cause continuous splitting and recombination, keeping the same flow path length for the two split streams. This SAR principle governs mixing at lower *Re*. As *Re* increases, the serpentine channel design starts to induce chaotic advection. Thus, efficient mixing in the SLM can be achieved for a wide range of *Re* ($0.44<Re<12.3$). Compared to a T-micromixer, the SLM design requires a 20-times shorter distance to achieve complete mixing. Later, an improved serpentine laminating micromixer (ISLM) was developed within the same group by Park *et al.*[57]. It was shown that the reduced cross-sectional area in the recombination region enhanced

the advection effect, which helped achieve better vertical lamination. This change results in improved mixing performance: at *Re* 0.2 and 20 at least a 1.2-fold shorter distance was required to achieve complete mixing for the ISLM compared to the SLM.

Xia *et al.*[58] designed and investigated several configurations of two-layer crossing channels in the micromixers (TLCCM, Fig. 4B). All three mixers have a two-layer structure. It is thought that the complex 3D geometry of the microchannels would impose perturbations on the flow. However, Model 1 fails to generate chaotic advection at Re<1, which can be attributed to a lack of fluid inertial effects. Model 2 was found to be only a partial chaotic mixer, exhibiting incomplete mixing at *Re*=0.01. On the other hand, rapid mixing can be achieved at *Re*<1 for Model 3. When *Re* increased to 10, the mixing became even better due to promotion of chaotic advection. Further improvement was observed at *Re*=60. Recently, several similar designs, namely a tangentially crossing channel mixer (Fig. 4C)[9] and a micromixer with XH-shaped and XO-shaped elements (Fig. 4D),[10] both utilizing the combination of SAR and chaotic advection, were proposed. Both of these designs give a good performance for mixing fluids are a wide range of Reynolds numbers, 0.1<*Re*<10 and 0.3<*Re*<60, respectively.

Another micromixer with 3D square-wave structures and cubic grooves (Fig. 4E), that expands *Re* to a wider range (30<*Re*<220), was proposed by Lin *et al.*[11] The main flow path of the micromixer has a square-wave shape in order to facilitate laminar flow recirculation by vortex generation, followed by stretching of these vortices in the cubic groove. The mixer shows good performances in the range of 0.675 - 4 mL/min flow rates. In addition, the proposed micromixer featured a stainless steel body, making it resistant to high temperature, high pressure, and strong corrosion, which can be beneficial in many analytical applications.

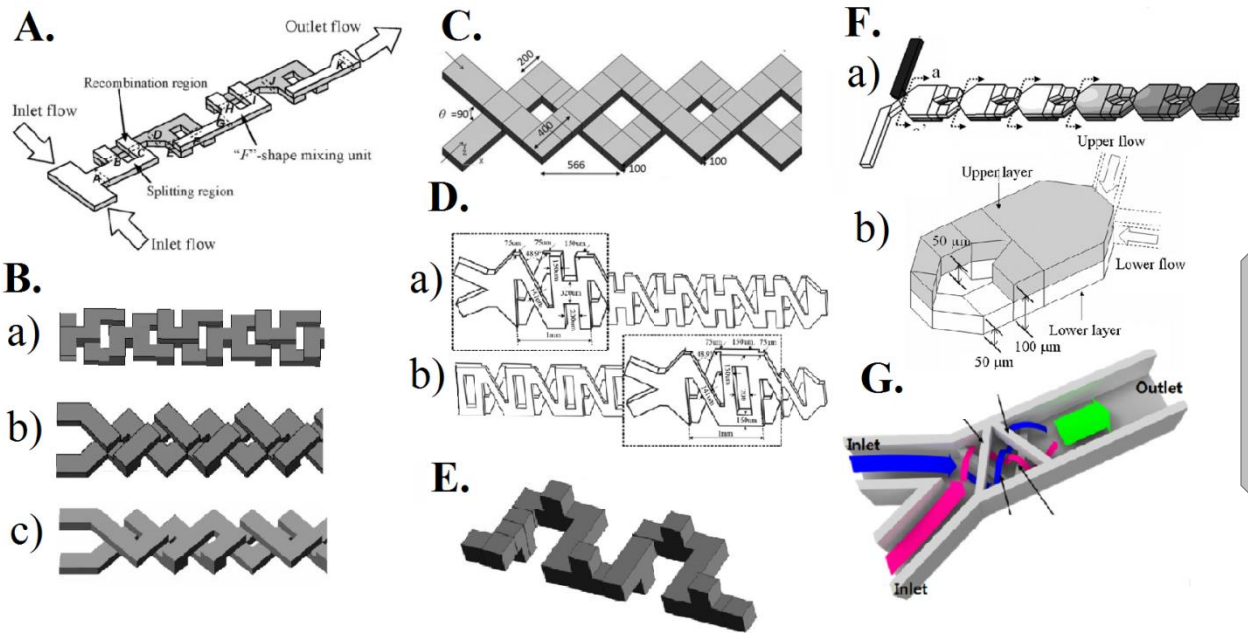

Figure 4. 3D convoluted channels: (A) Serpentine laminating micromixer (SLM) (Taken from[56]); (B) Configurations of two-layer crossing channels in the micromixer design: (a) Model 1, (b) Model 2 and (c) Model 3 (Modified from[58]); (C) Tangentially crossing channel (TCC) mixer (Modified from[9]); (D) SAR micromixer with (a) XH and (b) XO elements (Modified from[10]); (E) The micromixer with 3D square-wave structures and cubic grooves (Modified from[11]); (F) SAR μ-reactor (a) side view and (b) mixing unit (Modified from[59]); (G) Horizontal and vertical weaving micromixer (HVW mixer)(Modified from[12]). See Table 1 for geometric dimensions.

Fang and Yang[59] designed a SAR μ-reactor (Fig. 4F) suitable for mixing fluids with viscosities over a wide range (0.9–186 cP) for $0.01<Re<100$. The 3D structures inside the mixer cause stream cutting, separation and recombination utilizing the SAR principle. On the other hand, the mass transfer of fluids between upper and lower halves of the channel induces a 3D-counter-clockwise flow. The repetitive overlapping of flows forces them to collapse and stretch, which is a characteristic of chaotic advection. Results showed that at high flow rates, such as at $Re>50$, mixing becomes dominated by inertial forces and the complete mixing of fluids can be achieved within the first 6 mm of the length of the mixer. Furthermore, authors assessed the mixing behavior of fluorescent proteins (C-phycocyanin and R-phycoerythrin) in 88% glycerol with a confocal microscope. Results revealed that the SAR μ-reactor exhibit only a small difference (10–15%) in mixing efficiency when mixing highly viscous fluids (186 cP) as compared to slightly viscous fluids (0.9 cP). This difference for the micromixer with slanted grooves was 40–45%,[59] which indicates that the mixing of viscous fluids can be achieved more efficiently using a SAR μ-reactor.

Recently, a horizontal and vertical weaving micromixer (HVW mixer, Fig. 4G) with crossed barriers inside a microchannel was proposed.[12] Barriers cause two fluids to be divided into upper and lower layers followed by the generation of clockwise and counter clockwise motion both vertically and horizontally. The unique feature of this mixer is that only a very short distance of 450 μm is required, to obtain 89.9% mixing efficiency at a Reynolds number of 5. The overall channel width is 300 μm, channel depth is 200 μm and barrier dimensions were 50×100 μm (width by depth).

Another mixer for mixing fluids with widely different viscosities (in ratios of up to 10^4) has been reported by Xia *et al.*[15] The mixer with interconnected multi-channel network (Fig. 5A) also employs two mechanisms to improve the mixing. First, through splitting and recombination, the bulk fluid volumes are broken into thinner streams and chaotically recombined together. Afterwards, the multiple fluid streams enter a circular expansion chamber, where viscous flow instabilities lead to turbulent fluid motion. At flow rates higher than 0.20 mL/min, the initial occurrence of flow instability is observed. However, at lower flow rates, no flow instability occurs, which reduces the quality of mixing. The mixer was tested for mixing glycerol (680 cP) and other viscous samples (5440 cP, 17300 cP and 54600 cP) with aqueous solutions (~1 cP). As expected, the mixer becomes less efficient at increased viscosity ratios. However, complete mixing is still obtained by the end of the mixer (after 8 mixer units) for all tested mixtures.

Li *et al.*[13] developed an overbridge-shaped micromixer (OBM, Figure 5B) that was used for mixing two fluids under both isocratic and gradient conditions with *Re* values of 0.01-200 (Re_{cr}=10), corresponding to 0.0045 - 900 μL/min flow rates. The mixer was compared to the previously discussed SLM micromixer with F-shaped units [Fig. 4A],[56] which revealed that mixing performance of the OBM was always higher (>90%) comparing to F-shaped mixer (<60%) at the same Reynolds number. Numerical simulation showed that a mixing efficiency of more than 90% can be achieved for mixing fluids with different flow rate ratios ranging from 1:9 to 9:1, which can be useful in analytical and biological applications. The success of the OBM mixer can be explained by the combination of different designs used. The mixer consists of overbridge-shaped (OB) and square-wave (SW) channels. The OB channel has a branched structure, which split a single fluid stream into two sub-streams. One sub-stream flow together with the second fluid stream through the main SW channel, where the interface between streams is stretched at sharp turns. The other sub-stream is transported to the other side of the channel

and collided with the main stream at a 90° angle, which will increase the contact area between fluids.

Liu *et al.*[18] proposed a novel cross-linked dual helical micromixer (CLDH, Fig. 5C) that consists of double helical channels rotating in opposite directions to create repeated crossing regions. This mixer employs flow collision to stretch, split and fold streams that recombine in the crossing regions. Chaotic advection is enhanced with the sharply twisting streams on the basis of helical flow and flow collision where *Re*>1. The simulation and experimental results show that 99% mixing can be achieved in four cycles (320 μm) over a wide range of *Re* (0.003–30).

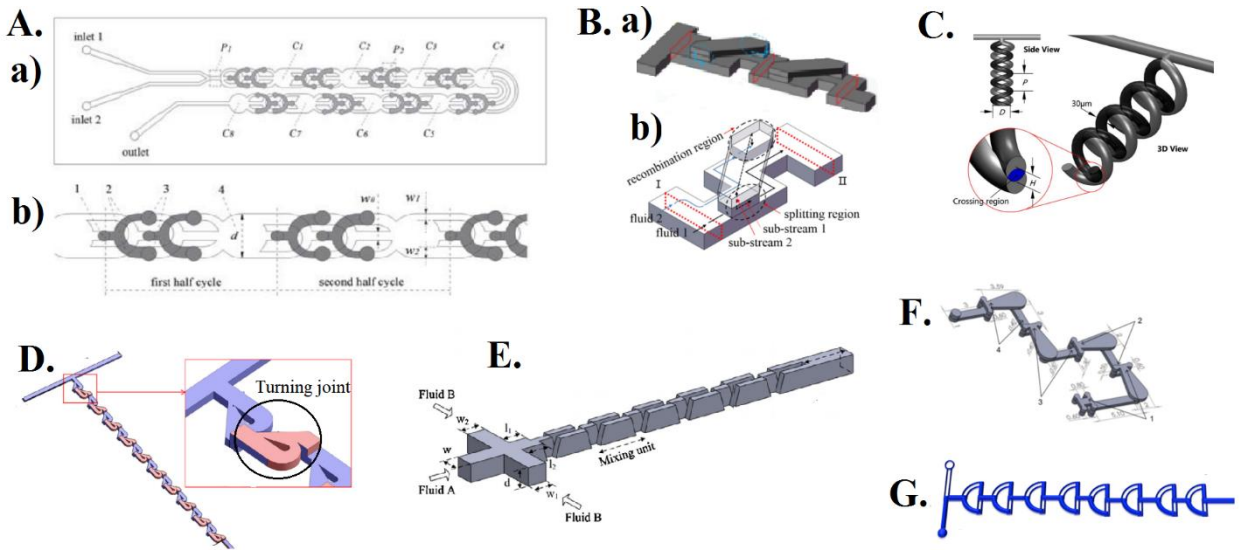

Figure 5. 3D convoluted micromixers. (A) (a) Plain view and (b) a profile of the mixer (Taken from[15]); (B) (a) 3-D overbridge-shaped micromixer (OBM) with (b) its mixing unit (Modified from[13]); (C) 3D cross-linked dual helical micromixer (CLDH) (Taken from[18]); (D) 3D Tesla micromixer (Modified from[19]); (E) Micromixer with shifted trapezoidal blades (STB) (Modified from[60]); (F) H-C passive micromixer (Modified from[20]); (G) "Twisted" 3D microfluidic mixer (Modified from[21]). See Table 1 for geometric dimensions.

Another possible approach for the creation of chaotic advection is the combination of Taylor dispersion with Dean vortices. Hong *et al.*[61] proposed to use an in-plane micromixer with modified Tesla structures. This mixer exploits the Coanda effect, which enhances convective mixing of the fluids by producing transverse Taylor dispersion. Recently, Yang *et al.*[19] designed a micromixer with three-dimensional Tesla structures (Fig. 5D). A repetitive distortion and squeezing of flow occurs at the turning joints of the Tesla structures that generate transverse dispersion. Moreover, an added layer of Tesla structures provides more flow disturbances, which improves mixing. The efficiency of mixing reached 94% in the flow rate

range of 0.9 - 900 μL/min (0.1<*Re*<100). The application of this mixer will be discussed in Section 4.2.2. Recently, another two micromixers were proposed for mixing in the similar range of *Re* (1<*Re*<100): a micromixer with shifted trapezoidal blades (STB, Figure 5E)[60] and an H-C micromixer (Fig. 5G)[20]. The mixing efficiency was 80% and 90%, respectively.

Sivashankar *et al.*[21] proposed a new "twisted" 3D microfluidic mixer with a two-layered quadrant of circles (Fig. 5F). Mixing is enhanced due to chaotic advection through generation of vortices at the edge of the arc-shaped channels, with additional splitting and recombination of flows. These micromixers can operate at low (1.0 μL/min) and high (1.0 mL/min) flow rates without reduction in the mixing performance. Moreover, the proposed mixer showed a good mixing efficiency at high flow rates for mixing 98% glycerol (919 cP) with water (1 cP), making this mixer ideal for a variety of applications where highly viscous solutions have to be mixed at high flow rates (~ 1.0 mL/min).

Table 1 summarizes different types of micromixers based on chaotic advection with their dimensions and material/fabrication methods. We highlighted the mixers from the current Section applications, which will be shown in Section 4. The lines in red colour marks the mixers that found a real application that was proposed in the original paper. The lines in blue highlights the application in which the original or modified mixer designs from the original study were used.

Table 1. Micromixers based on chaotic advection.

Name of the mixer	Re*	Dimensions	Material/fabrication method	Ref	Application area
CHAOTIC MICROMIXERS WITH SIMPLE GEOMETRIES					
Spiral S-shaped channel	0.02< *Re* < 18.6	w=150 μm; h = 29 μm	SEBS/ printed circuit technology; single planar soft lithography	35	A size-based particle filtration device;[86] a microreactor
Planar labyrinth micromixer (PLM) with S-shaped geometry	*Re* = 2.5; 30	h = 267 μm; w = 220 μm; the spacing - 240 μm	PDMS/single-step soft-lithography	5	
Spiral-shaped, interlocking-semicircle and Ω channel designs	0.01< *Re* < 50 Re_{cr} = 10	h = 230 μm; w = 200 μm; L = 22 mm	PDMS bonded to a glass/soft-lithography	6	for systems working under continuous flow conditions
Zig-zag channel	80< *Re* < 267 Re_{cr} = 80	h = 48 μm; w = 100 μm; L = 2 mm; s = 100-800 μm (s - periodic step)	Polyethyleneterephthalate (PET)/an excimer laser	36	A microreactor: polymerizations of styrene in cyclohexane; ultrasensitive trace analysis[62]
Curved-straight-curved (CSC) micromixer	*Re* = 1; 9; 81	w = 130 μm; h = 130 μm; L=1.95 mm; baffle thickness 40 μm; w(radial baffles) = 97.5 μm	PDMS bound to glass/soft lithography	27	As microreactor
Microchannels with lateral obstructions	Re_{cr} = 100	w = 50 μm; h = 50 μm (total); L = 66 mm;	SU-8 - PMMA/photolithography and micro-milling	22	In DNA hybridization analysis
Alcove-based mixer with a triangular obstruction	*Re* < 400	h = 82 μm; w = 20 μm; alcove: w = 30 μm; l = 40 μm	Silicon/standard photolithographic techniques	23	For handling complex biochemical and chemical reactions in parallel; mixing fluids with different viscosities
CHAOTIC MICROMIXERS WITH OBSTACLES IN THE MIXING CHANNEL					
Pillar obstruction channels	*Re:* 0.289-0.354 (0.1–15 μL/min) Re_{cr} ≥ 5 μL/min	h = 45 μm; w = 200 μm; L= 35 mml; pillars: h = 45 μm; w = 15 μm;	PDMS bound to glass/soft lithography	44	to mix solutions with different viscosities; [44] capturing bioparticles on the immobilized surfaces[85]
The obstruction micromixer with rectangular ribs	*Re* = 0.05	h = 50 μm; w = 100 μm	PDMS/soft lithography	26	Particle dispersion with a wide range of particle sizes[26]
Simple T-shaped-, T-shaped wavy- and T-shaped micro-channel with rectangular ribs	0.027 < *Re* < 0.081	w = 200 μm; h = 200 μm (total); L = 10.1 mm; obstacle sizes: w = 50 μm; l = 100 μm; h = 80 μm	PDMS – PDMS/two-step soft lithography	17	Capturing bioparticles on the immobilized surfaces
Mixers incorporating 2D and 3D baffles	0.1 < *Re* < 20 Re_{cr} = 1	w = 100 μm; h = 50 μm; L = 5.23 mm	PMMA- PMMA/an excimer laser beam	28	As microreactors; in DNA hybridization analysis
Microfluidic mixer with cylindrical alcoves or grooves (CG)	1 < *Re* < 10	w = 200 μm; h = 100 μm; r_{CG} = 100; 200; 300 μm; L = 20 mm	PDMS bound to glass/soft lithography	24	For biochemical and medical diagnosis
GROOVES IN THE CHANNEL					
Slanted groove micromixer (SGM)	0 < *Re* < 100	w = 200 μm; h = 70 μm; grooves: d = 14 μm	PDMS bound to glass/2-step soft lithography	52	A microreactor: synthesis of a statistical-copolymer-brush composition

					gradient;[63] continuous glucose monitoring;[72] on-line chemical modification of peptides and direct ESI-MS analysis[94]
Staggered herringbone mixer (SHM)		w = 200 μm; h = 77 μm; grooves: d = 17.7 μm			For parallel screening *in situ* click chemistry;[65] as microreactor: production of siRNA-LNPs[67–69] and continuous glucose monitoring;[71] trapping of particles and DNA hybridization;[75,82,83,84] trace analysis: sarin in blood[89] and cobalt (II) ions and hydrogen peroxide;[93] changing mobile phase composition between dimensions in LC×LC;[99] enzymatic digestion, one of the key functions of the gastrointestinal tract[100].
Grooves placed on the top and bottom of the channel	0.06 < *Re* < 10	w = 3.175 mm; h = 0.76; 1.02; 1.27 mm; d = 0.94 mm	PMMA – Plexiglas/milling	53	Binding reactions (for DNA extraction); trapping of particles; enrichment and focusing of beads and cells; in immunoassays (trapping cancer cells on the antibody-coated surface); in environmental analysis
	Re ≤ 30	w = 200 μm; h = 60 μm	PDMS/soft lithography	55	
Connected-groove micromixer (CGM)	0.28 < *Re* < 112	w = 200 μm; h = 70 μm; L = 1.7 mm; grooves: w = 50 μm; d = 30 μm	PDMS bound to glass/two standard photolithography	34	
Slanted ridge mixer (SRM)	*Re* ~ 1 (10 μL/min)	w = 185 μm (bottom); w = 120 μm (top); h = 90 μm; L = 43 mm; ridges: w = 70 μm; h = 20 μm	a glass plate bound to glass/two-step SU-8 process	7	
Three-dimensional staggered herringbone mixer (3D SHM)	*Re* ~ 0.7	w = 200 μm; h = 80 μm; grooves: h = 20 μm (bottom); h = 40 μm (side); w = 60 μm	fused silica bound to PDMS/femtosecond-laser-assisted chemical wet etching	8	
3D CONVOLUTED CHANNELS					
Serpentine laminating micromixer (SLM) with "F"- shape units	0.44 < Re < 12.3	w = 250 μm; h = 60 μm; L = 10 mm	COC/hot embossing; injection molding	56	In diagnostic devices (for blood typing);[88] in analytical chemistry and separation science (e.g., for gradients formation); as microreactor
Improved serpentine laminating micromixer (ISLM) with "F"- shape units	*Re* =0.2; 2; 20	w = 500 μm; h = 300 μm	PDMS bound to glass/soft lithography	57	
Two-layer crossing channels: TLCCM, model A and model B	0.01< *Re* < 0.2	w = 300 μm; h = 1500 μm	PMMA/the laser ablation method	58	As microreactors
Tangentially crossing channel (TCC) mixer	0.1 < *Re* < 10	w = 100 μm; h = 50 μm	PDMS-PDMS/soft lithography	9	
Micromixer with self-rotated contact surface (XH and XO models)	0.3 < *Re* < 60	w = 450 μm; h = 150 μm; L =10.25 mm	PDMS-PDMS/multilayer soft lithography	10	
SAR μ-reactor	0.01 < *Re* < 100	w = 300 μm; h = 100 μm; L =6.15 mm	PDMS/standard photolithography	59	Mixing of fluids with different viscosities[59]

Micromixer with 3D periodic perturbation	30 < *Re* < 220	h = 300 µm; L = 50 mm	stainless steel/conventional machining	11,101	In analytical chemistry (liquid chromatography); operations under pressure and temperatures
3D structures resembling teeth (alligator teeth-shaped micromixer)	0.08 < *Re* < 16	w = 300 µm; h = 100-300 µm, L = 20 mm; the triangular structures: w = 300 µm, h = 300 µm; d = 50, 100, 150 µm	PDMS-PDMS/soft lithography	64	as microreactors for continuous glucose monitoring,[64] DNA hybridization assays;[73,74,76,77] for an ultrasensitive trace analysis of cyanide[90]
3-D overbridge-shaped micromixer (OBM)	0.01 < *Re* < 200 Re_{cr}=10	w = 100 µm; h = 50 µm; L = 2 mm	Three layers of PDMS.single-step soft lithography	13	Formation of gradients (at different flow rate ratios)[13]
Horizontal and vertical weaving micromixer (HVW mixer)	*Re* = 5	w = 300 µm; h = 200 µm; L = 1.2 mm; barriers: w = 50 µm; d = 100 µm	PDMS – PDMS/soft lithography	12	Binding reactions (for DNA extraction); trapping of particles
A micromixer with interconnected multi-channel network	*Re* ~ 2.8 (400 µl/min)	w_1 = 600 µm, w_2 = 450 µm, w_3= 750 µm; h = 400 µm; $d_{chamber}$ = 3.45 mm.	PMMA – PMMA/CNC micro-milling	15	In analytical chemistry and separation science (e.g., for gradients formation)[15]
Micromixer with shifted trapezoidal blades (STB)	0.5 < *Re* < 100 Re_{cr} = 5	w = 210 µm; h = 200 µm	PDMS-glass/soft lithography	60	In clinical and environmental analyses or diagnostic systems
3D cross-linked dual helical micromixer (CLDH)	0.003 < *Re* < 30	D(helical)=60 µm; P(helical)=80 µm, separation distance: 21 µm	fused silica/femtosecond laser wet etching (FLWE) technology	18	-
Micromixer with modified Tesla structures	0.1 < *Re* < 100	w = 200 µm; h = 100 µm; L = 11.2 mm	PDMS/soft lithography	19	In immunofluorescence experiments (for binding reaction of antibodies for detecting antigens of lung cancer cells);[19] a microreactor: for fabrication of homogenous lipid-polymeric and lipid-quantum dot nanoparticles;[66] formation of gradients in liquid chromatography[95]
H-C passive micromixer	1, 30, 50, 100 Re_{cr} = 30	w_{max}= 600 µm, w_{min}= 400 µm; h_{max}= 1300 µm, h_{min}= 400 µm	PC/micromilling	20	-
"Twisted" 3D microfluidic mixer	0.02 < *Re* < 20 (1, 5, 10, 100, 1000 µL/min)	w = 200 µm; h = 200 µm; L = 30 mm	PMMA – PMMA/CO_2 laser system, thermal bonding	21	The mixing of various viscous fluids For diagnostic devices (cell analysis);[21] integrated systems for study of reaction kinetics, sample dilution, and improved reaction selectivity.

* Experimental values unless stated different.
The lines in red colour marks the mixers that found a real application that was proposed in the original paper. The lines in blue highlights the application in which the original or modified mixer designs from the original study were used. Other applications indicated in black are possible applications for each particular design.
PDMS - Poly(dimethylsiloxane); PC – Polycarbonate; COC – Cyclic olefin copolymer; PMMA – Poly(methyl methacrylate)
PETG - Polyethylene terephthalate glycol; SEBS - Polystyrene-Polyethylene-Polybutylene-Polystyrene

4. Application of the passive micromixers based on chaotic advection

Microfluidic systems are widely used in biology, biotechnology and chemistry. Most of these applications involve complicated (bio)chemical reactions that require mixing.[19] Micromixers based on chaotic advection have found their application as microreactors;[62–72] and in biological applications in the analysis of DNA,[73–81] sorting of particles and cells,[19,25,82–86] improvement of diverse cell culture platforms[87] and in full integrated lab-on-the-chip devices for blood typing[88] or for detecting a trace amount of sarin in whole blood.[89] In analytical chemistry chaotic micromixers have been used for analysis of hazardous compounds (*e.g.* cyanide, pesticides, malachite green);[89–93] on-line chemical modification of peptides in an LC-MS interface;[94] mixing liquids with different viscosities[15,21,44,59] and for gradient formation.[13,95]

4.1. Microreactors for chemical reactions

Micromixers as microreactors possess some unique features that are advantageous for using them for performing various chemical reactions. First, the microscale mixing time is usually equal to or even less than the reaction time. Of course, micromixers can not produce a large amount of product comparing to the macroscale production, however, the relative reaction yield can be higher and the synthesis can be performed in a more controllable way. Besides, in the micromixers the small thermal inertia and the uniform temperature provide improved control over mass and heat transfer.[1,65] This allows the synthesis of more homogeneous highly reproducible reaction products. The small volume of the microreactors also provides an opportunity for green syntheses by reducing the use of hazardous reagents, which makes the production more cost effective, and safe.[96] At the same time, the larger surface-to-volume ratio provides more surface for catalyst incorporation.

There are a few examples of utilizing chaotic mixers for polymerization reactions: a synthesis of a statistical-copolymer-brush composition gradient using a mixer with slanted grooves[63] and polymerizations of styrene in cyclohexane in zig-zag microchannels.[62] The flow rate in these applications was relatively high: ~0.15 - 0.3 mL/min. Both studies showed that the passive mixing induces by flow only allows more controllable processes in the microchannels, either for obtaining polymers with narrow molecular mass distribution[62] or for the fabrication of surface materials with well-defined composition gradients.[63]

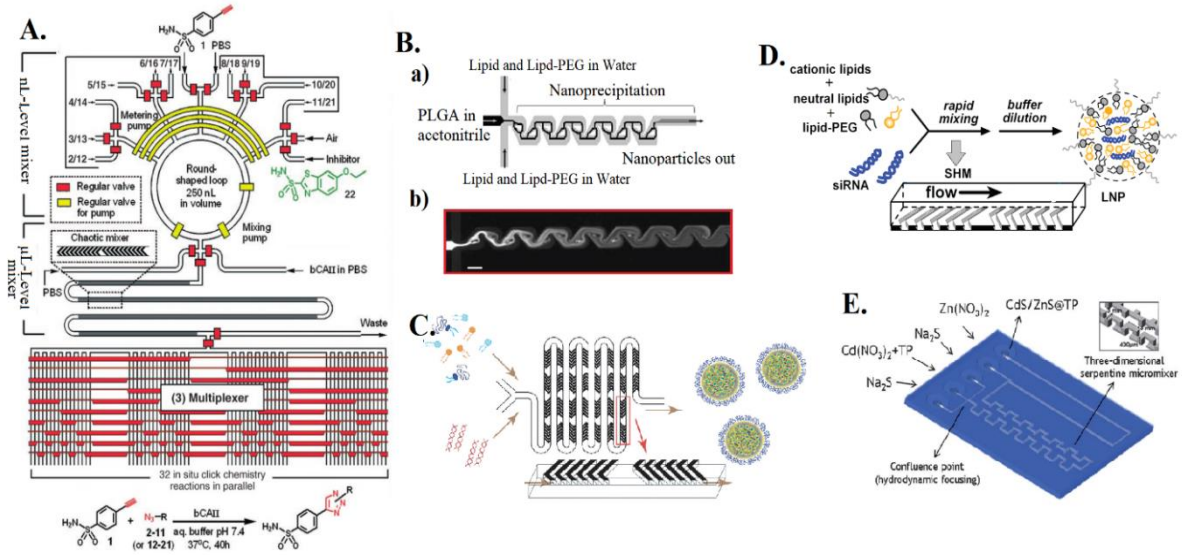

Figure 6. (A) Schematic representation of a chemical reaction circuit used for the parallel screening of an in situ click chemistry library (Adapted from[65]); (B) Schematic illustration of nanoprecipitation of lipid polymeric NPs (a) in microchannel with Tesla structures (discussed in Section 3.3) and (b) micrograph of mixing process between fluorescent dye and water at total flow rate 55 μL/min (Modified from[66]); (C) Schematic illustration of lipid nanoparticle (LNP) small interfering RNA (siRNA) formulation inside staggered herringbone micromixer (SHM) (Modified from[67,68]); (D) Schematic illustration of LNP formation in channel with groove structures for rapid mixing (Modified from[69]); (E) The ceramic microreactor design for the synthesis of core-shell nanocrystals with a three-dimensional serpentine micromixer for the formation of the core quantum dots and a longitudinal channel for the shell formation (Taken from[70]).

In 2006 Wang *et al.*[65] described a new type of microfluidics-based chemical reaction circuits for the parallel screening of 32 *in situ* click chemistry reactions. This approach allows to synthesize a library of high-affinity protein ligands from the complementary building block reagents via irreversible connection chemistry. In this work click reactions between acetylene and azide was chosen as a model system. Figure 6A shows how this performed in practice. First, a nanoliter-level rotary mixer (nL-Level mixer with a volume of 250 nL) selectively sample nL-quantities of reagents - acetylene and azides with/without inhibitors - for each screening reaction. Then, reagents enter the microliter-level chaotic mixer (μL-Level mixer) and mixed with mL-quantities of bovine carbonic anhydrase II (bCAII) solution by means of chaotic advection inside the 37.8-mm long microchannel. Afterwards, the homogeneous reaction mixtures are guided by microfluidic multiplexer into one of the 32 individually addressable microvessels for storing. As a result of these manipulations, 10 different binary azide/acetylene combinations are obtained: 1) ten *in situ* click chemistry reactions between

acetylene and azides in the presence of bCAII; 2) ten control reactions performed th same as in (1), but in the presence of inhibitor; 3) ten thermal click chemistry reactions performed as in (1), but in the absence of bCAII. The total volume of the system is only 4 μL, which allows to reduce the consumption of reagents in 2.5-11 times compared to the conventional method using 96-well plates.

A very good example of utilizing the micromixers as microreactors is their application for synthesis of lipid nanoparticles (LNP)[66] and their complexation with small interfering RNA (siRNA).[67–69] In order to obtain monodisperse LNP siRNA systems with minimum sizes that exhibit better gene silencing potency, faster mixing rates (higher flow rates) are required.[68] The conventional techniques for encapsulation of nucleic acids require milliliters of expensive nucleic acid solution and do not provide good homogeneity and reproducibility.[69] To overcome this, Valencia *et al.*[66] have developed a PDMS-based microfluidic mixer consisting of Tesla structures for fabrication of monodisperse homogenous lipid-polymeric and lipid-quantum dot nanoparticles (Fig. 6B). Other studies[67–69] have utilized a staggered herringbone mixer for production of siRNA-LNPs (Fig. 6C-D). Later, Rungta *et al.*[97] showed the efficient silence neuronal gene expression in cell culture and *in vivo* in the brain using LNPs produced this way.

Pedro *et al.*[70] have reported an automatic microreactor for the easy and controlled synthesis of water soluble quantum dots (CdS and CdS/ZnS) for *in situ* optical characterization. Homogeneous, stable and highly reproducible nanocrystals have been obtained due to a hydrodynamic focusing of reagents and the introduction of three-dimensional micromixers for efficient mixing (Fig. 6E).

Several studies used micromixers with staggered herringbone grooves,[71] slanted grooves[72] and three-dimensional structures resembling teeth[64] as microreactors for continuous glucose monitoring. For these experiments relatively low flow rates in the range of 0.37-75.0 μL/min were used. However, when the sample flow rate increases from 10 to 70 μL/min in a SHG mixer[71], a decrease in the detected signal was observed, apparently due to insufficient reaction times. On the other hand, in micromixers with three-dimensional structures[64] a mixing efficiency between 81% to 92% was determined for the full range of the tested flow rates (0.37-74.6 μL/min).

4.2. Biological applications

Biological processes, such as cell activation, enzyme reactions and protein folding, often involve reactions that require mixing of reactants for their initiation.[78]

4.2.1. DNA analysis

Nucleic acid (NA) probe assays have an enormous scope of applications in biotechnology and medicine in order to identify genes and mutants, to map their correlations, and to analyze their expression.[75,78] DNA microarrays involve multi-component biochemical reactions that use thousands of oligonucleotides, complementary DNA (cDNA) clones or polymerase-chain-reaction (PCR) products.[75] Therefore, the sample and reagents should be completely mixed in order to achieve good results. However, the fact that reagents are immobilized means that hybridization in the conventional way may take 8–24 hours due to the diffusion-limited kinetics.[73,75]

Recently, microfluidic devices started to attract attention for DNA probe assays due to their low costs, good performances, and ability to be used for different assays by just changing the nature of the reagents.[78] However, the fundamental problem faced by DNA-microarray in microfluidic devices remains: slow transport of DNA molecules to the probes at low Reynolds numbers.[75] To overcome this, many researchers have used microfluidic mixers based on chaotic advection. Several different designs of micromixers have been used for this application, including a three-dimensional serpentine mixer,[78,79] mixer with overlapping channels,[80] an alligator teeth-shaped micromixer[73,74,76,77] and mixer with herringbone grooves.[75]

Very often, modern diagnostic techniques require the isolation and purification of nucleic acids directly from patient samples. Several studies[78,79] reported utilization of three-dimensional serpentine micromixers for DNA extraction based on binding reaction to the glass surfaces. Lee *et al.* reported a DNA purification from a biological sample using a microfluidic mixer for a stepwise change in salt concentration.[79] Under high-salt buffer DNA, which is negatively charged, is strongly adsorbed on the glass surface. Afterwards, under a low-salt buffer conditions, adsorbed DNA was eluted from the glass. Due to the fact that other components of the sample (*e.g.* proteins or sugars) are weakly charged, DNA absorption occurs in a selective manner and allows its purification.

The group of S. Lee[73,74,76,77] had been working on the development of DNA hybridization assays using an alligator teeth-shaped PDMS microfluidic mixer (Figure 7A). The channel of this micromixers contains an array of upper and lower teeth that are responsible for the fluid dispersion of confluent streams in both transversal and vertical direction.[64] First, Park *et al.*[77] investigated the rapid and highly sensitive detection of duplex dye-labelled DNA sequences. A mixer was used for efficient mixing between DNA oligomers and aggregated

silver colloids and was operated under low flow rate of 0.37 - 74.6 μL/min. It should be noted that the mixing under the flow rate of 74.6 μL/min was not complete.

Later, Yea *et al.*[73] used an alligator teeth-shaped PDMS microfluidic channel for the lab-on-a-chip-based DNA hybridization analysis (Fig. 7B). The micromixer was used to obtain efficient mixing between the probe and target DNA oligomers at a flow rate of 1 μL/min. Kim *et al.*[76] and Jung *et al.*[81] then used a molecular beacon, a stem–loop DNA oligonucleotide labelled with two fluorescent dyes as a probe DNA to analyze a target DNA with 20 base pairs. Finally, Chen *et al.*[74] reported a fast and sensitive online detection technique for label-free target DNA based on changes in the FRET (Fluorescence Resonance Energy Transfer) signal resulting from the sequence-specific hybridization between two fluorescently labelled nucleic acid probes and target DNA in a PDMS microfluidic channel (Fig. 7C).

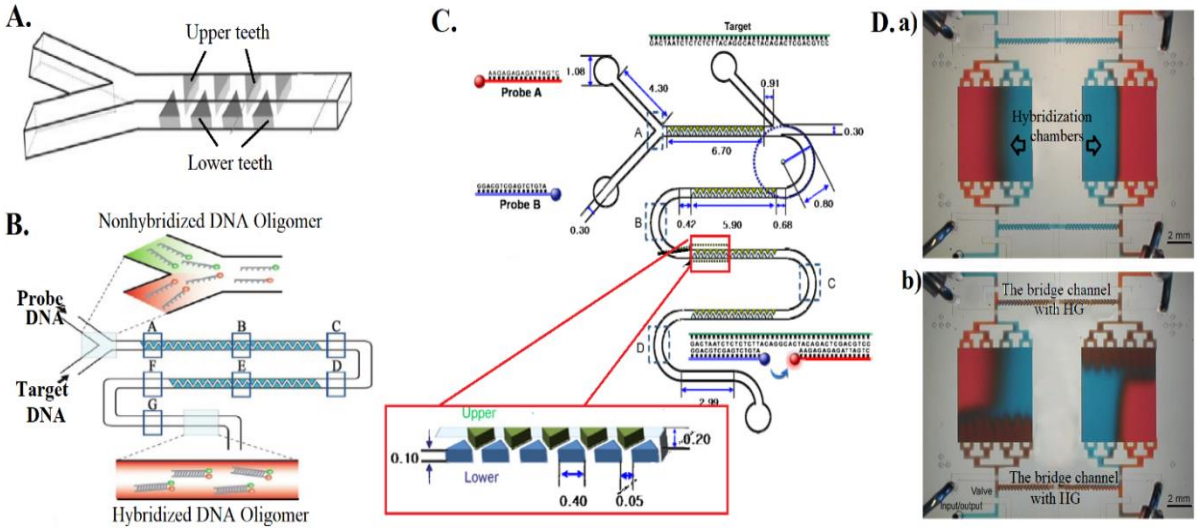

Figure 7. (A) Scheme of alligator teeth-shaped micromixer;[77] (B) Microfluidic channel for DNA hybridization with marked boxes for the FRET measurement areas (Adjusted from[73]); (C) (a) An alligator teeth-shaped mixer with (b) schematic drawing of an alligator-teeth-shaped channel,[91] that was used for DNA hybridization: two fluorescently labelled nucleic acid probes were mixed first, and then a target DNA oligonucleotide was added; (Modified from[74]); (D) (a) Optical micrographs of the PDMS device with two identical chambers, loaded half with red and half with blue solution, and (b) the situation when the pump start to circulate solution clockwise between chambers and the bridge channels with herringbone grooves (HG) provide mixing of red and blue solutions(Modified from[75]).

Another system for DNA hybridization (Fig. 7D) was constructed by Liu *et al.*[75] A microfluidic chip consisted of two identical hybridization chambers (6 × 6.5 × 65 mm, 5 mL) for solution circulation, which were connected to each other through the bridge channels with herringbone structure. When chambers are loaded with a sample and a peristaltic pump starts to circulate solution between chambers, the fluids passing through the bridge channels with

herringbone grooves experience chaotic advection which leads to their mixing. It takes about 16 min to complete the circulation between two chambers. In this device DNA hybridization was performed under dynamic and static (control) conditions using two identical PDMS devices. The cDNA samples were loaded into the PDMS devices and by actuating the peristaltic pumps in one of the devices a dynamic hybridization was performed, while static hybridization was performed in the other device as a control. After hybridization at 52°C for 2 h, PDMS devices were peeled away and scanned to recieve fluorescence images. It was observed that the hybridization in the dynamic conditions when microfluidic chaotic mixer was used, produced stronger signals and better sensitivity than under static conditions. Besides, it was demonstrated that a mixer with herringbone grooves enhances DNA hybridization signals 3-8-fold and improves sensitivity by nearly one order of magnitude relative to the conventional methods over the same length of time. The device is disposable and compatible with high-density microarray slides with a potential to hybridize about 135 000 array features in a single experiment.

4.2.2. Sorting/separation of particles and cells

Trapping, manipulation and separation of bioparticles (such as viruses, DNA molecules, bacteria, and cells) are important goals for biotechnology in order to develop a good therapeutic understanding of many diseases.[86] One way to achieve this is by using microconcentrators based on dielectrophoresis (DEP) for collecting these particles on electrodes. However, this approach is only effective, when the sample particles are brought close to electrode surfaces. Microfluidic mixers that generate a complex helical flow can recirculate particles and bring them closer to electrode surfaces (usually on the bottom of the channel) increasing the percentage of particles that get trapped. Lee and Voldman[82] designed a microconcentrator with patterned grooves to enhance the trapping of particles at high flow rate (100-500 μL/min), which also means that particle interaction with the electrode surface was strong (Fig. 8A). Different types of grooves – the slanted groove, staggered herringbone, and symmetrical herringbone mixers – were investigated. The amount of trapped particles (1-μm-size magnetic microspheres) in the staggered herringbone mixer increased by a factor of ~1.5x compared to a smooth channel. Here, the generation of vertical flow is even more important than achieving the mixing itself. Later, for enrichment and focusing of microbeads (6, 10, and 20 μm in diameter) and mouse dendritic cells, Chen *et al.*[25] used single slanted and V-shaped grooves under very low flow rate of 0.27 μL/min. Such a difference in the flow rate used is probably due to the lower efficiency of the symmetrical V-shaped grooves to generate vertical fluid

motion (and, thus, a longer residence time is required for trapping particles) comparing to the staggered herringbone mixer).

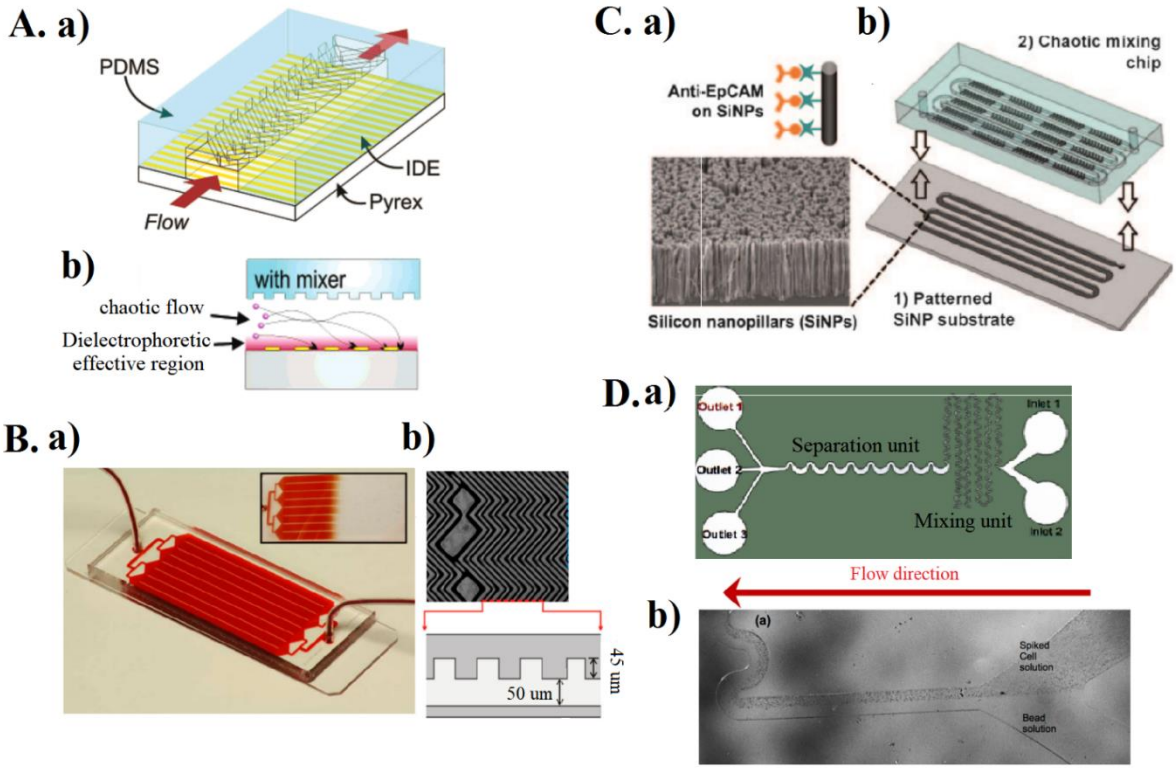

Figure 8. (A) (a) Illustration of the assembled device with a channel and gold interdigitated electrodes (IDEs) on the Pyrex substrate; (b) particle trapping in chaotic flow (Modified from[82]); (B) The HB-Chip with a microfluidic array of channels illustrating (a) the uniform blood flow through the device and (b) a micrograph of the grooved surface with a side view (Modified from[84]). (C) An integrated device for capturing circulating tumor cells (CTCs): (a) a patterned silicon nanopillar (SiNP) substrate with anti-EpCAM-coating, and (b) an overlaid microfluidic chaotic mixing chip (Modified from[85]); (D)(a)Schematic illustration of an integrated lab-on-a-disc system: two inlets, mixing unit and the connected inertial flow-focusing channel; (b) an upstream section of the mixing unit processing blood-spiked and microbead solutions (Taken from[86]).

Interestingly enough, a number of micromixers were used for the circulation of tumor cells by modifying the mixer surface. Idea of trapping particles come back in different applications. The group of Mehmet Toner[83,84] has reported a microvortex manipulator (MVM) with patterned chevrons (symmetrical V-shaped grooves) and herringbone grooves (asymmetric chevrons) on the upper wall. First, it was used for passive parallel focusing and guiding beads and cells[83] and then, for a platform of circulating tumor cells (CTC) isolation ("HB-Chip", Fig. 8B).[84] The HB-Chip design applies passive mixing of blood cells through the generation of microvortices in order to increase the number of interactions between target CTCs and the antibody-coated chip surface. The most unexpected finding of this study was the

isolation of CTCs clusters from the blood of patients with metastatic cancer, which may provide insight into the process of metastasis in human cancer.

Another CTC-capture platform was designed by Wang *et al.*[85] (Fig. 8C). It consists of a patterned silicon nanopillar (SiNP) substrate coated with cancer-cell capture agents (epithelial cell adhesion molecule antibody, anti-EpCAM) for recognizing/capturing EpCAM-expressing cells, and a PDMS chip with a serpentine mixer that contains chevron-shaped grooves. The last one induces a vertical flow in the microchannel that increases cell–substrate contact frequency resulting in enhanced CTC capture on SiNP substrate. The device was tested for blood samples from a prostate cancer patient and it showed significantly higher CTC numbers compared to the commercial CellSearch® assay.

Recently, Aguirre *et al.*[86] have demonstrated for the first time an integrated device for changing the properties of cells (by mans of complex creation) in order to separate them according to this property (size). The proposed device contains a micromixer for the creation of a cancer cell–microbead complex, and a flow-focusing region for separation (Fig. 8D). In addition to the mixing, provided by Dean flow, a chaotic advection is induced by turning the microchannel contents 180° at each turn (termed "flipping" by the authors). Depending on a size of a cancer cell–microbead complex, its trajectory will vary. Thus, the proposed system works as a size-based particle filtration device.

4.2.3. Fully-Integrated lab-on-the-chip devices

Mixers based on chaotic advection also found their application in microfluidic perfusion systems for cell culture studies.[87] The design of such generic systems with multiple functionalities that allows tuned and controllable (medium compositions, flow rates, gradients *etc.*) analysis of cell behaviour[87] is an attractive but challenging idea. In order to address the need for perfusion of large numbers of cells with the ability to change cell culture conditions, Cooksey *et al.*[87] developed a sophisticated system shown in Figure 9. It consists of closed-at-rest microvalves with a multiplexer (for combining of fluids), an on/off chaotic micromixer circuit, a bypass channel (to divert the flow to the waste output), a central chamber (containing three exits) and a novel microfluidic resistor (to control fluid flow rates). To achieve mixing, the device has a separate channel with deflectable herringbone-shaped PDMS membranes. Under negative pressure, membranes are deflected downward and become grooves that induce chaotic mixing (''on/off chaotic mixer''). If the chaotic mixer is bypassed, very little diffusive mixing occurs between the two coloured fluids. If the chaotic mixer is off (the grooves are not

actuated), the wide gradient is formed; if the mixer is turned on, the streams are completely mixed by the time they enter the chamber. This approach allows using the same device for generation of gradient as well as homogenized mixtures.

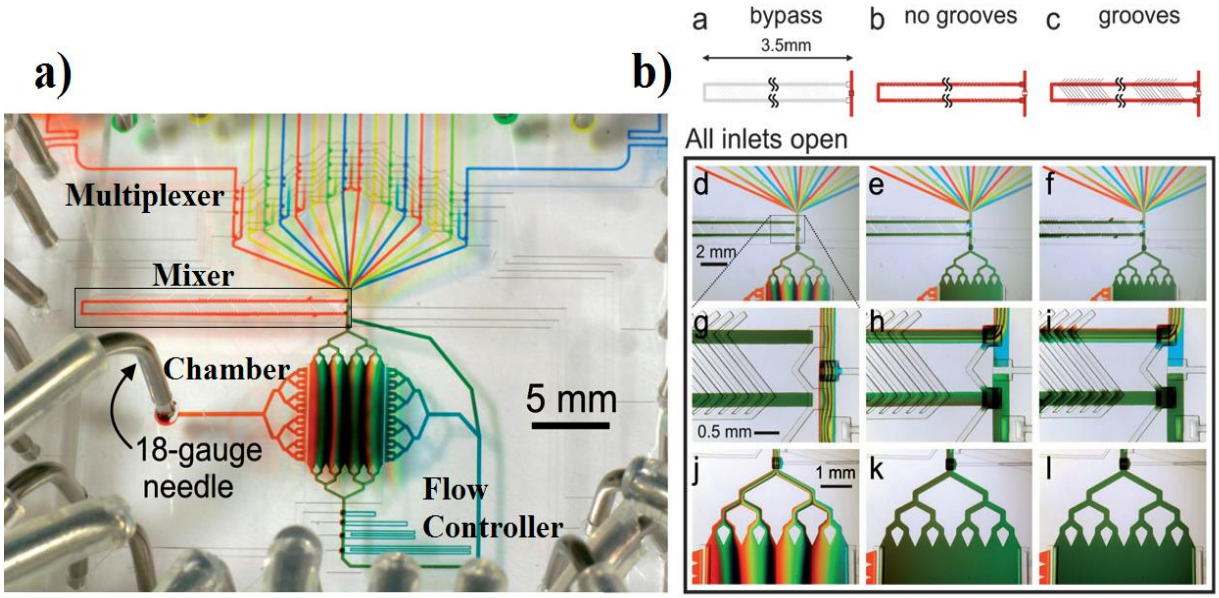

Figure 9. (a) Photograph of the device loaded with alternating colored inlets when all inlets are open; (b) different states and parts of on/off micromixer: herringbone mixer is bypassed (d,g,j)), herringbone membranes are undeflected (e,h,k), and grooves are activated (f,i,l) at 44 μL/min (Modified from[87]).

Kim *et al.*[88] designed an integrated microfluidic biochip for blood typing using both red blood cells (RBCs) and serum (Fig. 10). The reported lab-on-a-chip device consists of 4 parts: flow-splitting microchannels, chaotic micromixers, reaction chambers and detection microfilters. The sample blood (RBCs) and the standard serum are injected into the biochip through the flow splitting microchannels and are introduced into each connected chaotic micromixer for mixing. This induces the agglutination of RBCs with the corresponding antibodies. Then the mixture enters a reaction microchamber and stays there during the appropriate reaction time (1–3 min) for finishing the agglutination of RBCs. The reacted (or non-reacted) mixture of blood and serum passes through detection microfilters: the large size agglutinated RBCs are effectively filtered, whereas non-reacted RBCs easily pass through. The separation allows the visual detection of blood groups A, B, and AB with 3 μL of the whole blood within 3 min. A chaotic mixer used in this work is named serpentine laminating micromixer (SLM), that consists of eight ‘‘F’’-shaped mixing units (Section 3.3) that works under the flow rate of 30 μL/min.

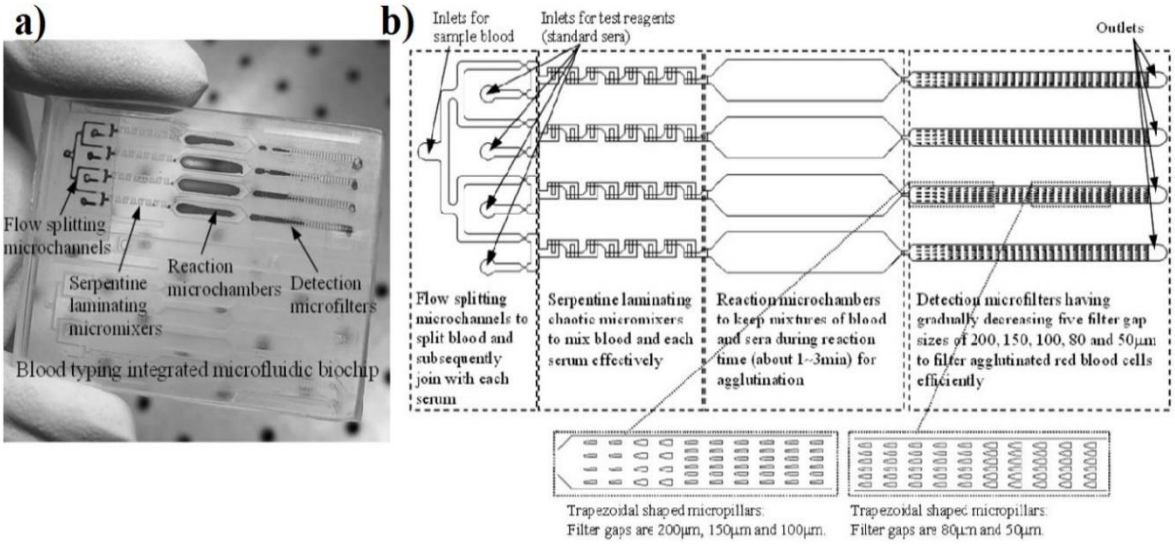

Figure 10. (a) Image of a blood typing microfluidic biochip and (b) schematic with flow splitting microchannels, chaotic micromixers, reaction microchambers and detection microfilters are fully integrated (Modified from[88]).

Tan *et al.*[89] fabricated a fully integrated lab-on-a-chip device for detecting a trace amount of sarin in a small volume of whole blood (Fig. 11). The chip consists of regeneration reactor for nerve agent regeneration from whole blood (realised as a micromixer); a channel with rectangular pillars for both reaction and filtration of precipitated blood proteins; a filter chamber with microbeads for removal of fluoride ions; an inhibition reactor (with the herringbone structures) for the enzyme-based hydrolysis reaction. The last section contains herringbone grooves to improve the transport of reagents to the immobilized surface coated with cholinesterase chromophore (enzyme) for the induced optical detection. For a longer shelf-life, the enzyme is protected by a coating layer. In this case, the coating layer is removed with an extra washing step before the measurement. If nerve agent exists in the blood sample, the enzyme is inhibited, hence hydrolysis of substrate is prevented and chromophore remained unconverted. The colour was determined by an absorbance measurement. The optimal flow rate was 20 μL/min, because enzymatic reaction requires longer time. When the flow rate was increased to 48 μL/min, only 5% of the enzymes were inhibited due to either inefficient mixing in the first two stages or insufficient residence time for the regeneration reaction. The rapid decrease in the efficiency is related to a relatively small volume of reaction chamber (63 μL comparing to the total volume of ~ 800 μL).

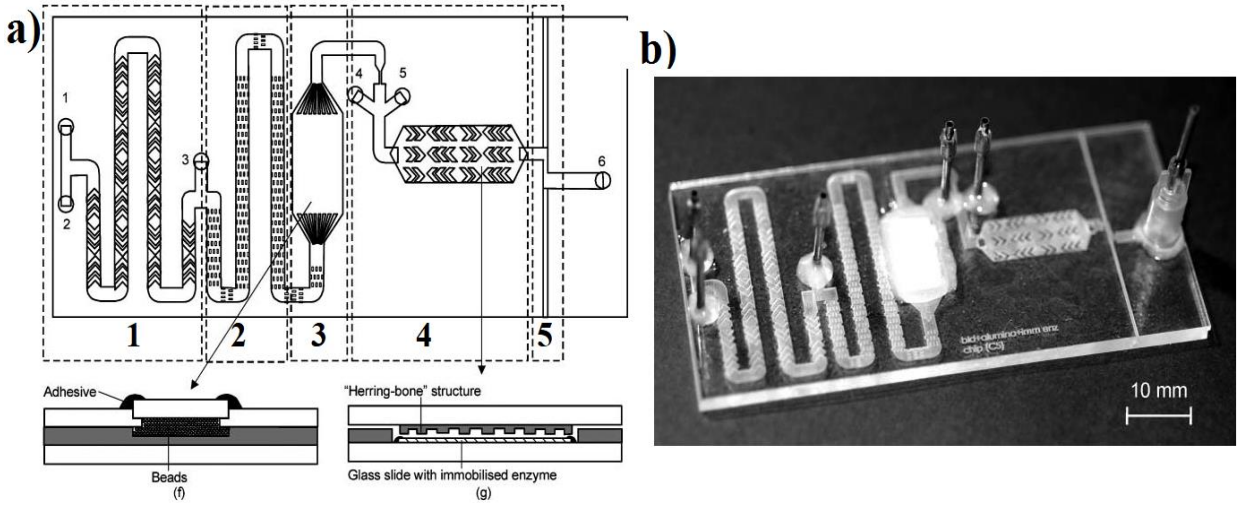

Figure 11. (a) Design of a lab-on-a-chip device for detection of nerve agent in blood consisting of (1) nerve agent regeneration reactor, (2) reaction and filtration channel; (3) a filter chamber with microbeads, (4) inhibition reactor with the herringbone structures and (5) optical detection region; and (b) the fabricated PMMA device. (Taken from[89]).

4.3. Analysis of hazardous compounds (environmental analysis)

Several groups had developed sensitive analytical systems for the detection of cyanide[90] and methyl parathion pesticides[91] in water, cyanide in the living cells[92] and cobalt (II) ions and hydrogen peroxide[93] using micromixers based on chaotic advection.

An already-mentioned micromixer – zig-zag-shaped microfluidic mixer with alligator teeth-shaped structures (Sec. 4.2.1)– was applied for development of an ultrasensitive trace analysis of cyanide[90] and methyl parathion pesticides[91] in water. In both studies, hazardous molecules were effectively adsorbed onto silver nanoparticles while flowing along the upper and lower parts of the channel (Fig. 12A). Both devices were fabricated in PDMS and investigated using confocal surface-enhanced Raman spectroscopy (SERS). The determined detection limits for methyl parathion pesticides and cyanide were 0.1 ppm and 0.5–1.0 ppb respectively. Later, Lee *et al.*[98] used the same system for the sensitive trace analysis for determining malachite green with limit of detection below the 1–2 ppb.

Kwon *et al.*[92] developed a fluorescent chemosensor, which exhibits a selective green fluorescence upon the addition of cyanide. In order to mix compounds, the mixing channel has herringbone-shaped obstacles on the wall that caused chaotic advection (Fig. 12B).

Developing a sensitive analytical system with a shorter analysis time, Lok *et al.*[93] presented a microchip containing a chaotic micromixer for luminol-peroxide chemiluminescence (CL) detection of cobalt (II) ions and hydrogen peroxide (as an artificial model system). The micromixer design was adopted from Tan *et al.*'s work[89] and consists of

forward and reversed staggered herringbone grooves (Figure 1CA), which allowed better catalytic interaction between the reactants. With a total volume of 145 µL, the corresponding residence time of the system ranges from 1.45 hours to 8.72 minutes at the flow rates from 1.67 to 16.7 µL/min respectively. The chip was also tested at 100 µL/min and 163 µL/min, which reduced the analysis times to 1.5 min and 1 min respectively. It was shown that a higher flow rate increases the CL intensity. However, it also leads to the excessive usage of reagents and leakages due to the increased pressure. As a compromise, the authors decided to use an optimal flow rate of 16.8 µL/min (analytical time of 8.65 min).[93]

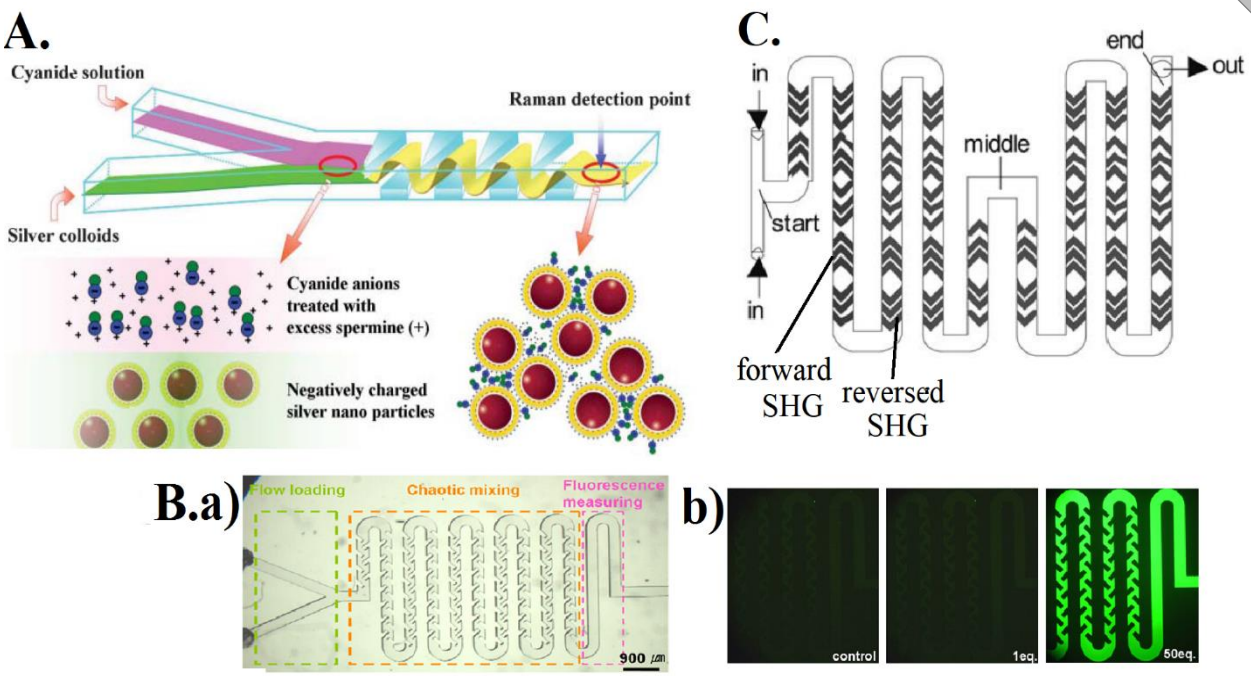

Figure 12. (A) An alligator teeth-shaped microfluidic mixer for mixing silver colloids and cyanide solution (Taken from[90]); (B) (a) Optical images of a fluorescent chemosensor (b) that exhibits a selective green fluorescence upon the addition of cyanide at a flow rate of 10 µL/min (Taken from[92]). (C) Schematic layout of the microchip with of forward and reversed staggered herringbone grooves (SHG) (Taken from [93]).

4.4. Analytical techniques

Recently, several interesting applications in the area of analytical chemistry were reported. Abonnenc *et al.*[94] explored the application of a new electrospray emitter microchip for on-line chemical modification of peptides and direct ESI-MS analysis (Fig. 13A). This microchip comprises a passive mixer with integrated photoablated slanted grooves to carry out on-chip chemical derivatization. In order to apply the voltage to the solution and consequently induce the ESI process, a carbon microelectrode is also integrated in the microchip. To illustrate the feasibility of the on-line tagging reaction directly on the electrospray microchip and to assess

the performance of such micromixer, on-chip chemical tagging of three cysteines with 1,4-benzoquinone was performed. As an ultimate application, the electrospray micromixer was implemented in an LC-MS workflow. It was shown that online derivatization of albumin tryptic peptides after a reversed-phase separation enhances the protein identification. Finally, on-line RPHPLC-tagging-ESI-MS of tryptic cysteinyl peptides of bovine serum albumin was achieved with the electrospray micromixer chip. In the present study, total flow rates from 4 to 6 µL/min were applied, at which good spray stability was demonstrated.

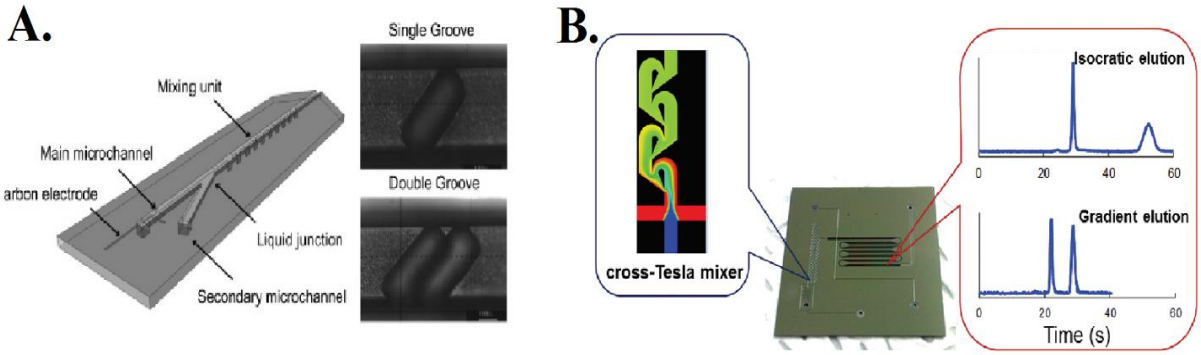

Figure 13. (A) Electrospray microchip with a mixing unit (Taken from[94]); (B) A gradient elution system for pressure-driven liquid chromatography on a chip and a photograph of the fabricated microchip with the cross-Tesla mixer (Modified from[95]).

In practice, biological and chemical samples vary over a wide range of their properties and some fluids that have to be mixed differ in viscosity. The viscosity differences can limit many processes in the microchannels (*e.g.* continuous chemical synthesis in microreactors, polymer formulation), and, thus, the utilization of a micromixer is essential. Several examples[15,21,44,59] of chaotic micromixers that were tested for mixing viscous fluids were presented in the Section 3.2 and 3.3. The utilization of these micromixers can be also useful in applications, where the differences in viscosity influence mixing dramatically (*e.g.* the high-viscous fluids can cause a dramatic increase of pressure in HPLC).

Another way to use micromixers for improving analytical techniques is in the formation of gradients.[13,95] One promising example - an overbridge-shaped micromixer[13] - was already presented in Section 3.3. Another mixer with integrated Tesla structure for formation of a gradient, a channel of pillar array columns for separation and a sample injection channel (Figure 13B) was proposed by Song *et al.*[95]. It was used for gradient elution of four aliphatic amines in pressure-driven reversed-phase liquid chromatography separation, that were successfully separated within 110 s at a total flow rate of 1.0 µL/min.. Due to the gradient elution conditions, the separation was shorter with sharper peaks than under isocratic elution

conditions. These micromixers have great potential in the improvement of conventional techniques combined with microfluidic technology, especially in the analysis of complex biological samples.

In our group, we developed a pressure-resistant microfluidic mixer with herringbone grooves for changing the mobile phase composition between two columns in on-line comprehensive two-dimensional liquid chromatography (LC×LC).[99] The device is meant to mix in-line rapidly in the wide range of flow rates (0.1-1 mL/min). This chip was micromilled in rigid cyclic-olefin copolymer (COC) and can withstand pressures of 200 bar due to a specially designed low-dead-volume interface. Using standardized HPLC connectors, the chip is directly connected to LC×LC system. It was successfully implemented for improved separation and identification of various oligomeric series in polyamide samples and showed similar performance to the commercially available mixing units.

5. Discussion

In the Section 3 the reader was already introduced to the Table 1, which summarizes different types of micromixers based on chaotic advection with their dimensions and material/fabrication methods. This table can serve as a good guideline for helping scientists to make a right choice of appropriate mixer. However, in this chapter we are also providing the reader with the detailed process of choosing the micromixer taking into account many aspects of the requirements set by the particular application (Figure 14).

There are a lot of different micromixers proposed in the literature that were developed for a specific application, however there is no a straightforward approach for choosing an appropriate micromixer for a particular application. Besides, the same micromixer can be successfully used for a variety of applications (Table 1, last column). However, it is possible to draw some general criteria that should be taken into account while choosing an appropriate mixer design among a big number of existing micromixers. The first thing that should be done is to define clear requirements for the particular application. It is important to know what kind of samples (chemical, biological etc.), ranges of flow rates (or residence times) and detection methods will be used (Fig. 14). The application will also dictate choice of substrate material or fabrication of the mixer. For example, some hydrophobic molecules can be absorbed in PDMS. In combination with three-dimensional convoluted micromixers, the produced insoluble materials in chemical synthesis[102] or biological material in bio-applications can easily clog the PDMS chip.

Another important criterion is the required flow rate range. It also dictates the material of the mixer (and, thus, a fabrication method) and the type of connection with the macro world. Most microfluidic systems are operated under low flow rates (0.2-75 μL/min). Therefore, those micromixers can be fabricated in PDMS/PDMS or PDMS/glass by soft lithography (Table 1). However, in cases where higher flow rates (0.9 - 4 mL/min) and/or the connection to conventional equipment (*e.g.* LC, MS) are necessary, microfluidic systems have to be fabricated from more rigid materials (e.g. PMMA, silicon, stainless steel) and appropriate pressure-resistant connectors are needed, to resist higher pressures. The choice of the material influences the type of fabrication method that should have a sufficient resolution for fabrication of a particular design.

The detection method that is planned to be used, also determines the material (*e.g.* devices should be transparent in case of optical detection), the required flow rate and the type of connection with other equipment (if applicable). For example, the signal intensity in chemiluminescent detection relies on the speed of mixing that determines the sensitivity of the method. The higher flow rate in this case provides not only the faster analysis, but what is more important a control over degree of dispersion of reactive species to localize the reaction region. This increases the intensity of the chemiluminescent signal and, therefore, the method sensitivity. This requires the utilization of micromixers that can mix at relatively high flow rates (>100 μL/min).

When the flow rate range is set and the material is chosen, it is possible to decide which type of micromixer (simple geometry, obstacles/wall modifications or 3D convoluted channels) will be the most efficient under the defined flow conditions. As mentioned in the beginning of this chapter, flow conditions (described by *Re*), under which the mixer operates, dictate the type of phenomena that govern mixing (dominance of diffusion or advection). This means that each type of mixer has its own range of flow rates under which it shows the best performance. There are similar patterns in mixing performances in all mixers: below some critical value of Re, the mixing efficiency decreases with the increase of flow rate (dominance of diffusion); and above this value the mixing efficiency increases with the increase of flow rate (dominance of chaotic advection).

Besides those patterns some micromixers have inherent features that are especially beneficial for particular applications. For example, micromixers with patterned grooves can be used in applications, where reactants have to be trapped on the immobilized surfaces (*e.g.*, on electrodes[82]). In this case grooves on both top and bottom channel walls facilitate the binding reactions[85,86] not only because of the ability to mix reactants, but also due to the creation of the vertical flow (in the z-direction) that provides better transport of reactants to the immobilized surfaces. This approach can be used for analysis of bioparticles with lower diffusivity (*e.g.* proteins, DNA),[75] which have to be transported faster to the probes than just by diffusion. Other examples are micromixers with simple geometries (*e.g.* spiral, zig-zag, serpentine). They can work under a wide range of Reynolds numbers ($1 << Re < 800$) due to the appearance of vortices, which resulted in mixing by chaotic advection at high Re and molecular diffusion at low Re. This type of mixers contains long channel paths and, thus, provides long residence time for efficient mixing of reactants to form the final product. These features make them suitable to be used as microreactors or for DNA hybridization.

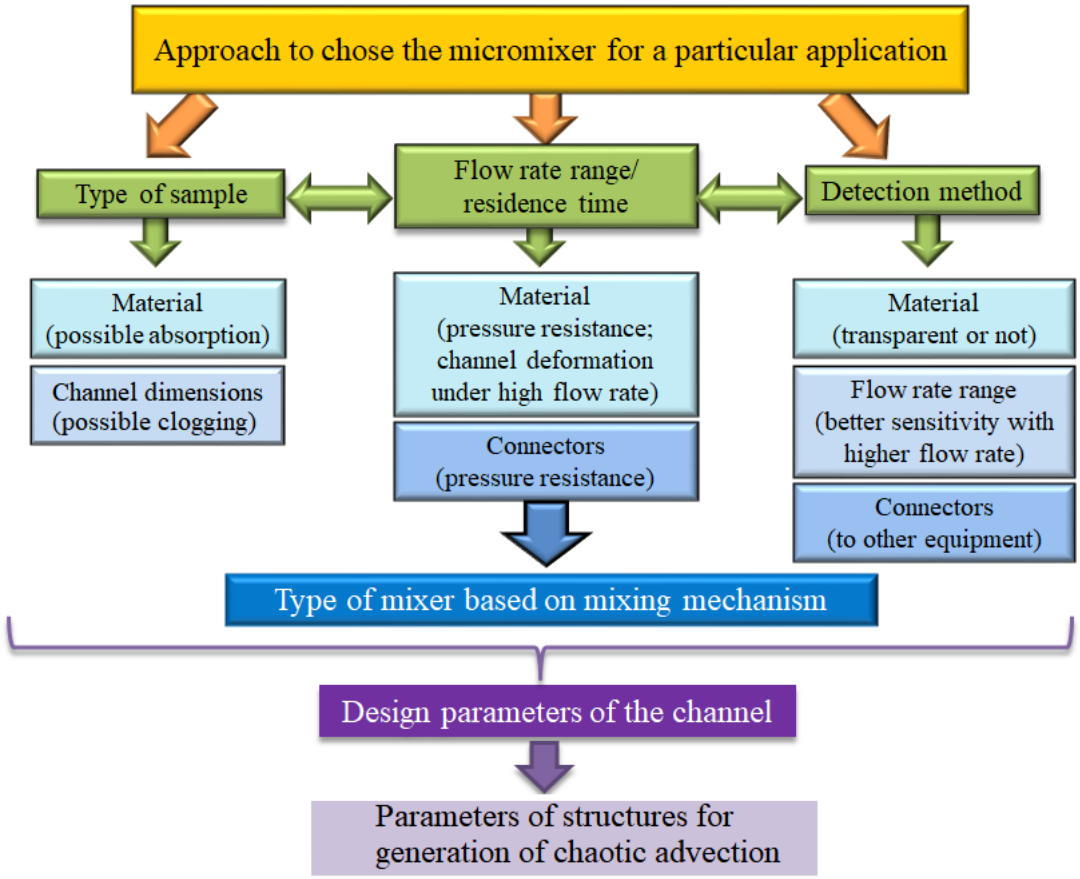

Figure 14. The approach for choosing the chaotic micromixer for a particular application.

Although mixers with obstructions in the channel are used in a smaller range of *Re* (0.01<Re< 80), they can also be used for the same purposes as mixers with simple geometries due to the increase of the reactants residence time in the obstruction region.[22] Besides, the ability to modify the obstructions (*e.g.* micropillars) inside the mixer with reacting agents opens a wide range of possibilities for separation and extraction processes, for example when the analytes of interest are trapped on micropillars (*e.g.* DNA capturing or detection of affinity binding in immunoassays).

However, the same design features that are beneficial to some applications can impose negative effects at the same time. For instance, very deep grooves can create a large dead volume or force reactant to stay too long in the groove, which distorts peak shape in the chromatographic separation. Furthermore, the perpendicular bends of 3D convoluted designs can create dead volume zones (the fluid at the corner of these bends is stagnant, the only mass transport is diffusion).

After choosing the type of chaotic micromixer, it is important to draw an appropriate design taking into account all nuances related to the channel parameter and the design of the structures (obstructions, grooves *etc*). The geometry of the structures placed in the mixing channel is described by their depth, width, the angle position, symmetrical or asymmetrical arrangment *etc*. A larger depth and width of obstructions leads to a higher chance for inducing chaotic advection by creating larger vortices in the flow streamlines, which increases larger contact area between two flows. For instance, studies[50,85] showed that the mixing in micromixers with staggered herringbone grooves improves with deeper grooves. This can be explained by the increased fluid entrainment in the grooves leading to an increase of the vertical motions of the fluid at the side edges of the groove.[47]

The number of obstructions placed in the channel also influences the mixing performance.[9] For instance, Wang *et al.*[42] investigating cylindrical pillars in a mixing channel found that the mixing improves with the increase of the number of obstacles in the channel (within same area). Sahu *et al.*[22] also observed that mixing efficiency increases quadratically with the number of obstructions. The authors explained this observation by fluids staying in the obstruction region for a longer time (with larger number of obstruction), which provides more time to finish mixing by diffusion.

Hence, in order to make a choice of an appropriate micromixer that performs the best way possible for a particular application, many criteria should be considered. This choice should be done in consideration with all nuances related to the type of the sample, the flow rate range and the unique features of the application. However, the amount and the variety of already available designs ease this task. There is no need to develop completely new micromixers, it is enough to choose a right design and alter it towards the needs of a specific application.

6. Conclusions

In this chapter, we showed novel designs of passive micromixers based on chaotic advection that were proposed within the last decade. We classified them according to their geometry: simple geometries, mixers with obstacles in the channel or wall modification, and 3D convoluted channels. The chaotic micromixers with simple planar geometries provide better mixing at $Re>10$, because the Dean flow that governs mixing is intensified with the increase of the flow rate. The introduction of obstructions to the channel and pattering the channel wall with grooves provide the efficient mixing at lower Re ($0.01<Re<80$ and $1<Re<100$, respectively). The mixing in a wider range of Reynolds numbers ($0.1<Re<260$) is achieved, when the mixers with 3D convoluted channels are used due to the combination of two mixing mechanisms: SAR and chaotic advection.

We showed successful applications of passive chaotic mixers in chemical industry, biology and analytical chemistry. Most of applications described in this chapter use the range of flow rates from 0.01 μL/min to 4 mL/min. Micromixers based on chaotic advection have found their application as microreactors, in analysis of DNA, in sorting of particles and cells, to improve diverse cell culture platforms and in the full integrated lab-on-the-chip devices. In analytical chemistry chaotic micromixers were used for analysis of hazardous compounds (*e.g.* cyanide, pesticides, malachite green), for an on-line chemical modification of peptides in a LC-MS interface, for mixing liquids with different viscosities, for gradient formation or improving the performance of conventional analytical techniques such as LC×LC.

As it was shown in this chapter, very often, a mixer having a particular design finds diverse applications in a number of different areas. As an example we can name a mixer with herringbone grooves[52] (we report here 13 different applications)[65,67–69,71,75,82–84,89,93,99,100] or an alligator teeth-shaped micromixer[64] (with 6 applications).[64,73,74,76,77,90] These micromixers can be used in a such big variety of ways due to the fact that they work efficiently in a wide range of flow rates.

We hope that this chapter will prove to be useful for the scientists in their endeavours with respect to choosing and implementation of appropriate micromixers to the real-world applications.

References

1. Nguyen, N.-T. & N.-T. Nguyen. *Micromixers: Fundamentals, Design and Fabrication*. *Igarss 2014* (William Andrew Publishing, 2011). doi:10.1016/B978-1-4377-3520-8.00001-2
2. Capretto, L., Wei Cheng, M. H. & Zhang, X. Micromixing Within Microfluidic Devices. *TripleC* **304,** 27–68 (2011).
3. Nguyen, N.-T. & Wu, Z. Micromixers—a review. *J. Micromechanics Microengineering* **15,** R1–R16 (2005).
4. Lee, C. Y., Wang, W. T., Liu, C. C. & Fu, L. M. Passive mixers in microfluidic systems: A review. *Chem. Eng. J.* **288,** 146–160 (2016).
5. Li, P., Cogswell, J. & Faghri, M. Design and test of a passive planar labyrinth micromixer for rapid fluid mixing. *Sensors Actuators, B Chem.* **174,** 126–132 (2012).
6. Al-Halhouli, A. *et al.* Passive micromixers with interlocking semi-circle and omega-shaped modules: Experiments and simulations. *Micromachines* **6,** 953–968 (2015).
7. Van Schijndel, T. *et al.* Toward gradient formation in microfluidic devices by using slanted ridges. *Macromol. Mater. Eng.* **296,** 373–379 (2011).
8. Lin, D. *et al.* Three-dimensional staggered herringbone mixer fabricated by femtosecond laser direct writing. *J. Opt.* **15,** 025601 (2013).
9. Lee, D. & Lo, P. H. On the enhancement of mixing in tangentially crossing micro-channels. *Chem. Eng. J.* **181–182,** 524–529 (2012).
10. Feng, X., Ren, Y. & Jiang, H. An effective splitting-and-recombination micromixer with self-rotated contact surface for wide Reynolds number range applications. *Biomicrofluidics* **7,** 1–10 (2013).
11. Lin, Y., Yu, X., Wang, Z., Tu, S. T. & Wang, Z. Design and evaluation of an easily fabricated micromixer with three-dimensional periodic perturbation. *Chem. Eng. J.* **171,** 291–300 (2011).
12. Yoo, W.-S., Go, J. S., Park, S. S.-H. & Park, S. S.-H. A novel effective micromixer having horizontal and vertical weaving flow motion. *J. Micromechanics Microengineering* **22,** 5007 (2012).
13. Li, X., Chang, H., Liu, X., Ye, F. & Yuan, W. A 3-D Overbridge-Shaped Micromixer for Fast Mixing Over a Wide Range of Reynolds Numbers. *J. Microelectromechanical Syst.* **24,** 1391–1399 (2015).
14. Chen, Z. *et al.* Performance analysis of a folding flow micromixer. *Microfluid. Nanofluidics* **6,** 763–774 (2009).
15. Xia, H. M., Wang, Z. P., Koh, Y. X. & May, K. T. A microfluidic mixer with self-excited 'turbulent' fluid motion for wide viscosity ratio applications. *Lab Chip* **10,** 1712–1716 (2010).
16. The, H. Le *et al.* Geometric effects on mixing performance in a novel passive micromixer with trapezoidal-zigzag channels. *J. Micromechanics Microengineering* **25,** 094004 (2015).
17. Hsieh, S.-S. & Huang, Y.-C. Passive mixing in micro-channels with geometric variations through μPIV and μLIF measurements. *J. Micromechanics Microengineering* **18,** 065017 (2008).
18. Liu, K. *et al.* Design and analysis of the cross-linked dual helical micromixer for rapid mixing at low Reynolds numbers. *Microfluid. Nanofluidics* **19,** 169–180 (2015).
19. Yang, A. S. *et al.* A high-performance micromixer using three-dimensional Tesla structures for bio-applications. *Chem. Eng. J.* **263,** 444–451 (2015).
20. Viktorov, V., Mahmud, M. R. & Visconte, C. Design and characterization of a new H-C passive micromixer up to Reynolds number 100. *Chem. Eng. Res. Des.* **108,** 152–163 (2016).
21. Sivashankar, S. *et al.* A 'twisted' microfluidic mixer suitable for a wide range of flow rate applications. *Biomicrofluidics* **10,** 034120 (2016).
22. Sahu, P. K., Golia, A. & Sen, A. K. Investigations into mixing of fluids in microchannels with lateral obstructions. *Microsyst. Technol.* **19,** 493–501 (2013).
23. Egawa, T., Durand, J. L., Hayden, E. Y., Rousseau, D. L. & Yeh, S. R. Design and evaluation of a passive alcove-based microfluidic mixer. *Anal. Chem.* **81,** 1622–1627 (2009).
24. Wang, L., Liu, D., Wang, X. & Han, X. Mixing enhancement of novel passive microfluidic mixers with cylindrical grooves. *Chem. Eng. Sci.* **81,** 157–163 (2012).
25. Chen, H.-H., Sun, B., Tran, K. K., Shen, H. & Gao, D. A microfluidic manipulator for enrichment and alignment of moving cells and particles. *J. Biomech. Eng.* **131,** 074505 (2009).
26. Bhagat, A. A. S. & Papautsky, I. Enhancing particle dispersion in a passive planar micromixer using rectangular obstacles. *J. Micromechanics Microengineering* **18,** 085005 (2008).
27. Tsai, R. T. & Wu, C. Y. An efficient micromixer based on multidirectional vortices due to baffles and channel curvature. *Biomicrofluidics* **5,** 1–13 (2011).
28. Conlisk, K. & Connor, G. M. O. Analysis of passive microfluidic mixers incorporating 2D and 3D baffle geometries fabricated using an excimer laser. *Microfluid. Nanofluidics* **12,** 941–951 (2012).
29. Malvern Instruments Worldwide, *Understanding Taylor Dispersion Analysis* (2015).

30. Pidugu, S. B. & Bayraktar, T. FLOW PHYSICS IN MICROCHANNELS. in *Proceedings of IMECE2005 2005 ASME International Mechanical Engineering Congress and Exposition* 1–6 (2005).
31. Aref, H. Stirring by chaotic advection. *J. Fluid Mech.* **143,** 1–21 (1984).
32. Tai, C. H. *et al.* Micromixer utilizing electrokinetic instability-induced shedding effect. *Electrophoresis* **27,** 4982–4990 (2006).
33. Yan, D., Yang, C., Miao, J., Lam, Y. & Huang, X. Enhancement of electrokinetically driven microfluidic T-mixer using frequency modulated electric field and channel geometry effects. *Electrophoresis* **30,** 3144–3152 (2009).
34. Yang, J. T., Fang, W. F. & Tung, K. Y. Fluids mixing in devices with connected-groove channels. *Chem. Eng. Sci.* **63,** 1871–1881 (2008).
35. Sudarsan, A. P. & Ugaz, V. M. Fluid mixing in planar spiral microchannels. *Lab Chip* **6,** 74–82 (2006).
36. Mengeaud, V., Josserand, J. & Girault, H. H. Mixing processes in a zigzag microchannel: Finite element simulations and optical study. *Anal. Chem.* **74,** 4279–4286 (2002).
37. Nguyen, N. T. & Wereley, S. Fundamentals and applications of microfluidics. *Artech House* 111 (2006). doi:http://doi.wiley.com/10.1002/1521-3773%252820010316%252940%253A6%253C9823%253A%253AAID-ANIE9823%253E3.3.CO%253B2-C
38. Bothe, D., Stemich, C. & Warnecke, H. J. Fluid mixing in a T-shaped micro-mixer. *Chem. Eng. Sci.* **61,** 2950–2958 (2006).
39. Hoffmann, M., Schlüter, M. & Räbiger, N. Experimental investigation of liquid-liquid mixing in T-shaped micro-mixers using μ-LIF and μ-PIV. *Chem. Eng. Sci.* **61,** 2968–2976 (2006).
40. Ait Mouheb, N., Malsch, D., Montillet, A., Solliec, C. & Henkel, T. Numerical and experimental investigations of mixing in T-shaped and cross-shaped micromixers. *Chem. Eng. Sci.* **68,** 278–289 (2012).
41. Park, J. M., Seo, K. D. & Kwon, T. H. A chaotic micromixer using obstruction-pairs. *J. Micromechanics Microengineering* **20,** 015023 (2010).
42. Wang, H., Iovenitti, P., Harvey, E. & Masood, S. Optimizing layout of obstacles for enhanced mixing in microchannels. *Smart Mater. Struct.* **11,** 662 (2002).
43. Kang, T. G., Singh, M. K., Kwon, T. H. & Anderson, P. D. Chaotic mixing using periodic and aperiodic sequences of mixing protocols in a micromixer. *Microfluid. Nanofluidics* **4,** 589–599 (2008).
44. Chen, L. *et al.* Evaluation of passive mixing behaviors in a pillar obstruction poly(dimethylsiloxane) microfluidic mixer using fluorescence microscopy. *Microfluid. Nanofluidics* **7,** 267–273 (2009).
45. Hossain, S., Ansari, M. A., Husain, A. & Kim, K. Y. Analysis and optimization of a micromixer with a modified Tesla structure. *Chem. Eng. J.* **158,** 305–314 (2010).
46. Hessel, V., Löwe, H. & Schönfeld, F. Micromixers—a review on passive and active mixing principles. *Chem. Eng. Sci.* **60,** 2479–2501 (2005).
47. Lynn, N. S. & Dandy, D. S. Geometrical optimization of helical flow in grooved micromixers. *Lab Chip* **7,** 580–587 (2007).
48. Tóth, E., Holczer, E., Iván, K. & Fürjes, P. Optimized Simulation and Validation of Particle Advection in Asymmetric Staggered Herringbone Type Micromixers. *Micromachines* **6,** 136–150 (2015).
49. Chen, F. *et al.* Process for the fabrication of complex three-dimensional microcoils in fused silica. *Opt. Lett.* **38,** 2911–4 (2013).
50. Yang, J.-T., Huang, K.-J. & Lin, Y.-C. Geometric effects on fluid mixing in passive grooved micromixers. *Lab Chip* **5,** 1140–1147 (2005).
51. Yun, S., Lim, G., Kang, K. H. & Suh, Y. K. Geometric effects on lateral transport induced by slanted grooves in a microchannel at a low Reynolds number. *Chem. Eng. Sci.* **104,** 82–92 (2013).
52. Stroock, A. D. *et al.* Chaotic mixer for microchannels. *Science* **295,** 647–651 (2002).
53. Howell Jr., P. B. *et al.* A microfluidic mixer with grooves placed on the top and bottom of the channel. *Lab Chip* **5,** 524–530 (2005).
54. Hardt, S., Drese, K. S., Hessel, V. & Schönfeld, F. Passive micromixers for applications in the microreactor and ??TAS fields. *Microfluid. Nanofluidics* **1,** 108–118 (2005).
55. Floyd-Smith, T. M., Golden, J. P., Howell, P. B. & Ligler, F. S. Characterization of passive microfluidic mixers fabricated using soft lithography. *Microfluid. Nanofluidics* **2,** 180–183 (2006).
56. Kim, D. S., Lee, S. H., Kwon, T. H. & Ahn, C. H. A serpentine laminating micromixer combining splitting/recombination and advection. *Lab Chip* **5,** 739–747 (2005).
57. Park, J. M., Kim, D. S., Kang, T. G. & Kwon, T. H. Improved serpentine laminating micromixer with enhanced local advection. *Microfluid. Nanofluidics* **4,** 513–523 (2008).
58. Xia, H. M., Shu, C., Wan, S. Y. M. & Chew, Y. T. Influence of the Reynolds number on chaotic mixing in a spatially periodic micromixer and its characterization using dynamical system techniques. *J. Micromechanics Microengineering* **16,** 53–61 (2006).

59. Fang, W. F. & Yang, J. T. A novel microreactor with 3D rotating flow to boost fluid reaction and mixing of viscous fluids. *Sensors Actuators, B Chem.* **140,** 629–642 (2009).
60. Le The, H. *et al.* An effective passive micromixer with shifted trapezoidal blades using wide Reynolds number range. *Chem. Eng. Res. Des.* **93,** 1–11 (2015).
61. Hong, C.-C., Choi, J.-W. & Ahn, C. H. A novel in-plane passive microfluidic mixer with modified Tesla structures. *Lab Chip* **4,** 109–113 (2004).
62. Iida, K. *et al.* Living anionic polymerization using a microfluidic reactor. *Lab Chip* **9,** 339–345 (2009).
63. Xu, C. *et al.* Solution and surface composition gradients via microfluidic confinement: Fabrication of a statistical-copolymer-brush composition gradient. *Adv. Mater.* **18,** 1427–1430 (2006).
64. Kim, D. J., Oh, H. J., Park, T. H., Choo, J. B. & Lee, S. H. An easily integrative and efficient micromixer and its application to the spectroscopic detection of glucose-catalyst reactions. *Analyst* **130,** 293–298 (2005).
65. Wang, J. *et al.* Integrated microfluidics for parallel screening of an in situ click chemistry library. *Angew. Chemie - Int. Ed.* **45,** 5276–5281 (2006).
66. Valencia, P. M. *et al.* Single-step assembly of homogenous lipid-polymeric and lipid-quantum dot nanoparticles enabled by microfluidic rapid mixing. *ACS Nano* **4,** 1671–1679 (2010).
67. Leung, A. K. K. *et al.* Lipid nanoparticles containing siRNA synthesized by microfluidic mixing exhibit an electron-dense nanostructured core. *J. Phys. Chem. C* **116,** 18440–18450 (2012).
68. Belliveau, N. M. *et al.* Microfluidic Synthesis of Highly Potent Limit-size Lipid Nanoparticles for In Vivo Delivery of siRNA. *Mol. Ther. Nucleic Acids* **1,** e37 (2012).
69. Chen, D. *et al.* Rapid discovery of potent siRNA-containing lipid nanoparticles enabled by controlled microfluidic formulation. *J. Am. Chem. Soc.* **134,** 6948–6951 (2012).
70. Pedro, S. G. *et al.* A ceramic microreactor for the synthesis of water soluble CdS and CdS/ZnS nanocrystals with on-line optical characterization. *Nanoscale* **4,** 1328 (2012).
71. Xu, Z. R. & Fang, Z. L. Composite poly(dimethylsiloxane)/glass microfluidic system with an immobilized enzymatic particle-bed reactor and sequential sample injection for chemiluminescence determinations. *Anal. Chim. Acta* **507,** 129–135 (2004).
72. Moon, B. U., De Vries, M. G., Cordeiro, C. A., Westerink, B. H. C. & Verpoorte, E. Microdialysis-coupled enzymatic microreactor for in vivo glucose monitoring in rats. *Anal. Chem.* **85,** 10949–10955 (2013).
73. Yea, K., Lee, S., Choo, J., Oh, C.-H. & Lee, S. Fast and sensitive analysis of DNA hybridization in a PDMS micro-fluidic channel using fluorescence resonance energy transfer. *Chem. Commun. (Camb).* 1509–1511 (2006). doi:10.1039/b516253j
74. Chen, L. *et al.* DNA hybridization detection in a microfluidic channel using two fluorescently labelled nucleic acid probes. *Biosens. Bioelectron.* **23,** 1878–1882 (2008).
75. Liu, J., Williams, B. A., Gwirtz, R. M., Wold, B. J. & Quake, S. Enhanced signals and fast nucleic acid hybridization by microfluidic chaotic mixing. *Angew. Chemie - Int. Ed.* **45,** 3618–3623 (2006).
76. Kim, S. *et al.* Rapid DNA hybridization analysis using a PDMS microfluidic sensor and a molecular beacon. *Anal. Sci.* **23,** 401–405 (2007).
77. Park, T. *et al.* Highly sensitive signal detection of duplex dye-labelled DNA oligonucleotides in a PDMS microfluidic chip: confocal surface-enhanced Raman spectroscopic study. *Lab Chip* **5,** 437–442 (2005).
78. Yun, K.-S. & Yoon, E. Microfluidic Components and Bio-reactors for Miniaturized Bio-chip Applications. *iotechnology Bioprocess Eng. 2004* **9,** 86–92 (2004).
79. Lee, N. Y., Yamada, M. & Seki, M. Development of a passive micromixer based on repeated fluid twisting and flattening, and its application to DNA purification. *Anal. Bioanal. Chem.* **383,** 776–782 (2005).
80. Fang, W. F., Hsu, M. H., Chen, Y. T. & Yang, J. T. Characterization of microfluidic mixing and reaction in microchannels via analysis of cross-sectional patterns. *Biomicrofluidics* **5,** 1–12 (2011).
81. Jung, J. *et al.* Fast and sensitive DNA analysis using changes in the FRET signals of molecular beacons in a PDMS microfluidic channel. *Anal. Bioanal. Chem.* **387,** 2609–2615 (2007).
82. Lee, H. Y. & Voldman, J. Optimizing micromixer design for enhancing dielectrophoretic microconcentrator performance. *Anal. Chem.* **79,** 1833–1839 (2007).
83. Hsu, C.-H., Di Carlo, D., Chen, C., Irimia, D. & Toner, M. Microvortex for focusing, guiding and sorting of particles. *Lab Chip* **8,** 2128–2134 (2008).
84. Stott, S. L. *et al.* Isolation of circulating tumor cells using a microvortex-generating herringbone-chip. *Proc. Natl. Acad. Sci.* **107,** 18392–18397 (2010).
85. Wang, S. *et al.* Highly Efficient Capture of Circulating Tumor Cells by Using Nanostructured Silicon Substrates with Integrated Chaotic Micromixers. *Angew. Chemie Int. Ed.* **50,** 3084–3088 (2011).
86. Aguirre, G. R., Efremov, V., Kitsara, M. & Ducrée, J. Integrated micromixer for incubation and separation of cancer cells on a centrifugal platform using inertial and dean forces. *Microfluid. Nanofluidics* **18,** 513–526 (2015).

87. Cooksey, G. A., Sip, C. G. & Folch, A. A multi-purpose microfluidic perfusion system with combinatorial choice of inputs, mixtures, gradient patterns, and flow rates. *Lab Chip* **9,** 417–26 (2009).
88. Kim, D. S., Lee, S. H., Ahn, C. H., Lee, J. Y. & Kwon, T. H. Disposable integrated microfluidic biochip for blood typing by plastic microinjection moulding. *Lab Chip* **6,** 794–802 (2006).
89. Tan, H. Y., Loke, W. K., Tan, Y. T. & Nguyen, N.-T. A lab-on-a-chip for detection of nerve agent sarin in blood. *Lab Chip* **8,** 885–891 (2008).
90. Yea, K. *et al.* Ultra-sensitive trace analysis of cyanide water pollutant in a PDMS microfluidic channel using surface-enhanced Raman spectroscopy. *Analyst* **130,** 1009–1011 (2005).
91. Lee, D. *et al.* Quantitative analysis of methyl parathion pesticides in a polydimethylsiloxane microfluidic channel using confocal surface-enhanced Raman spectroscopy. *Appl. Spectrosc.* **60,** 373–377 (2006).
92. Kwon, S. K. *et al.* Sensing cyanide ion via fluorescent change and its application to the microfluidic system. *Tetrahedron Lett.* **49,** 4102–4105 (2008).
93. Lok, K. S., Kwok, Y. C. & Nguyen, N.-T. Passive micromixer for luminol-peroxide chemiluminescence detection. *Analyst* **136,** 2586–91 (2011).
94. Abonnenc, M., Dayon, L., Perruche, B., Lion, N. & Girault, H. H. Electrospray micromixer chip for on-line derivatization and kinetic studies. *Anal. Chem.* **80,** 3372–3378 (2008).
95. Song, Y. *et al.* Integration of pillar array columns into a gradient elution system for pressure-driven liquid chromatography. *Anal. Chem.* **84,** 4739–4745 (2012).
96. Krishna, K. S., Li, Y., Li, S. & Kumar, C. S. S. R. Lab-on-a-chip synthesis of inorganic nanomaterials and quantum dots for biomedical applications. *Adv. Drug Deliv. Rev.* **65,** 1470–1495 (2013).
97. Rungta, R. L. *et al.* Lipid Nanoparticle Delivery of siRNA to Silence Neuronal Gene Expression in the Brain. *Mol. Ther. Nucleic Acids* **2,** e136 (2013).
98. Lee, S. *et al.* Fast and sensitive trace analysis of malachite green using a surface-enhanced Raman microfluidic sensor. *Anal. Chim. Acta* **590,** 139–144 (2007).
99. Ianovska, M. A. *et al.* Microfluidic micromixer as a tool to overcome solvent incompatibilities in two-dimensional liquid chromatography.
100. Haan, P. de *et al.* "Digestion-on-a-Chip: A Continuous-Flow Modular Microsystem for Enzymatic Digestion for Gut-on-a-Chip Applications. (2018).
101. Lin, Y. Numerical characterization of simple three-dimensional chaotic micromixers. *Chem. Eng. J.* **277,** 303–311 (2015).
102. Bally, F., Serra, C. A., Hessel, V. & Hadziioannou, G. Micromixer-assisted polymerization processes. *Chem. Eng. Sci.* **66,** 1449–1462 (2011).